Mathematical Modelling of the Transmission Dynamics of Cholera

by

MWAURA STEPHEN NDUNGU

Submitted in accordance with the requirements for the degree of

MASTER OF SCIENCE

in

APPLIED MATHEMATICS

at the

UNIVERSITY OF SOUTH AFRICA

SUPERVISOR: Prof. Justin M. W. Munganga

Submission: January 2024

Declaration

Name: Mwaura Stephen Ndungu

Student number: 36260738

Degree: MSc. (Applied Mathematics)

Thesis Title: **Mathematical Modelling of the Transmission Dynamics of Cholera**

I declare that the above dissertation is my own work and that all the sources that I have used or quoted have been indicated and acknowledged by means of complete references.

I further declare that I submitted the dissertation to originality checking software and that it falls within the accepted requirements for originality.

I further declare that I have not previously submitted this work, or part of it, for examination at UNISA for another qualification or at any other higher education institution.

_   _

SIGNATURE   **DATE**

Dedication

I wish to dedicate this dissertation to my family for their support throughout the period of the study.

Acknowledgments

I thank God Almighty for good health during the time I have been working on this dissertation. I thank my supervisor, Prof. J. M. W. Munganga, for his patience and guidance throughout the research.

TABLE OF CONTENTS

List of Tables

List of Figures

Abstract

In the present research, analysis of a mathematical model of cholera which includes vaccinated individuals was performed. It is proved that if control reproduction number $\mathcal{R}_C < 1$, a suitable Lyapunov function is used to establish the global stability of the disease free equilibrium, which means that the disease will die out over time. Global stability analysis shows that when $\mathcal{R}_C < 1$, there exists at least one endemic equilibrium. If $\mathcal{R}_C > 1$, there exists a unique endemic equilibrium which is globally asymptotically stable. Sensitivity analysis of parameters indicates that the ingestion rate β of *Vibrio cholerae* by humans due to contact with contaminated sources greatly influences $\mathcal{R}_C$ followed by rate of natural loss of *Vibrio cholerae*, μ_B. An extension of the model to include possible optimal control strategies targeting to reduce β such as hygiene and improved sanitation are considered. Numerical simulations indicate that the number of infected individuals reduces when controls are in place to reduce ingestion of cholera pathogens, which shows that control measures are effective.

KEY TERMS

Cholera Modelling; SEIR Model; Disease Free Equilibrium; Control Reproduction Number; Global Stability; Local Stability; Lyapunov Function; Optimal Control; Pontryagin's Maximum Principle; Hamiltonian Function

Chapter 1

Introduction

1.1 Cholera

Cholera is an infectious diarrhoeal disease caused by a bacterium called *Vibrio cholerae*. The germs live in water mostly along the coastal regions. Although there are hundreds of strains/serogroups of cholera pathogens, only serogroups 01 and 0139 are known to cause epidemics [41]. It is estimated that globally there are 1.3 to 4.0 million cholera cases and 20,000 to 145,000 cholera deaths per year [74]. During 2022, WHO reported 472 697 cases and 2349 deaths from 44 countries [2]. The current cholera pandemic (seventh) has impacted over 120 countries, mostly in less developed regions. Millions of cases are never reported [74].

A renowned British Scientist, John Snow (1813-1858), has been widely acknowledged as the father of modern epidemiology due to his systematic approach in seeking answers to disease issues in London. After qualifying as a medical doctor at the University of London in 1844, Snow was admitted into the Royal College of Physicians in 1850 [95]. With determination to understand the epidemic of 1854, he carefully mapped cholera cases in London and identified contaminated water from a public well pump as the source of the disease [26]. Following his recommendations, the pump was removed and cholera cases dropped immediately. Snow successfully dismissed the "bad air" (miasma) theory as the cause of cholera. Snow recognized that disease treatment requires looking at individual patients within the larger community and the environment they live in [16].

This approach helps in understanding infectious diseases to this day. Snow's efforts to understand cholera are summarized below [24]:

1831: An epidemic strikes London. Therapeutic approaches then were not effective against cholera. Before disappearing in 1832, 50,000 Britons had died.

1848: Another epidemic strikes. Two successive cholera deaths from the same residence were reported.

1849: Snow is convinced cholera was spread through contaminated water.

1853: Snow had collected enough data that linked cholera to specific water supplies.

1.1.1 Vibrio Cholerae

The organism causing cholera was unknown until Pacini (1812-1883) and Koch (1843-1910) [45] came up with its description as highlighted below:

1884: Filippo Pacini, a germ theory believer, took interest in cholera. After examining different cholera victims, he discovered a bacterium in the intestines and called it *vibrio*.

1884: Robert Koch, who had earned worldwide fame for discovering tuberculosis bacillus in 1881, came up with the name *vibrio cholerae* as the germ that was responsible for cholera spread. Over time, works of Snow, Pacini and Koch convinced other physicians that "miasma" theory, which refers to bad air in the environment, was not relevant to cholera spread [111].

1.1.2 Cholera Outbreaks and Pandemics

In the last two centuries, cholera pandemics have hit mankind seven times, with the first recorded one originating from India in 1817 [88]. The strains responsible for the first four pandemics are unknown, but the fifth and the sixth ones are associated with *Vibrio Cholerae* OI classical biotype. There has been no clear criteria for distinguishing one pandemic period from the other and different researchers have given different descriptions for different pandemics [88]. Table 1.1 displays a brief schedule of cholera outbreaks and pandemics upto the current one which is said to have started in 1961.

Table 1.1: Cholera Outbreaks and Pandemics [58]

Pandemic	**Period**	**Approximate Deaths**
First	1817-1824	200,000
Second	1829-1837	450,000
Third	1846-1860	2 Million
Fourth	1863-1875	1 Million
Fifth	1881-1896	900,000
Sixth	1899-1929	1.5 Million
Seventh	1961-1975	100,0000

1.1.3 Cholera Spread

Cholera primarily spreads through consumption of contaminated water or food. Contaminated water sources, inadequate sanitation and poor hygiene contribute to transmission [68]. Additionally, person-to-person transmission can occur in crowded or unsanitary living conditions. The bacterium thrives in aquatic environments, especially in regions with warm temperatures [68]. Factors such as floods, heavy rains or natural disasters can lead to contamination of water sources, escalating the risk of cholera outbreaks.

Cholera can be transmitted through consumption of raw or undercooked seafoods, particularly in areas where it is endemic [87]. Shellfish, in particular, can harbour the bacteria, posing a risk to individuals who consume them. Inadequate sanitation infrastructure and poor hygiene practices significantly contribute to the spread of cholera. Lack of access to clean water, improper waste disposal and insufficient sanitation facilities create environments conducive to bacterial growth and transmission [87]. Over the years, three cholera waves have spread widely to different parts of the world. These waves have caused untold suffering especially in developing countries where levels of hygiene and sanitaty conditions are relatively low. Figure 1.1 shows the different directions of the waves as per the seventh pandemic phylogenetic tree.

Cholera can be introduced to new regions through international travels [22]. Infected individuals or contaminated goods can carry the bacterium across borders, leading to outbreaks in areas that may not have previously experienced cholera. High population density areas, especially in urban slums or refugee camps with limited access to clean water and sanitation facilities create conditions conducive to rapid cholera transmission. Proximity facilitates person-to-person spread. Cholera often exhibits seasonal patterns, with increased prevalence during the warmer months [31].

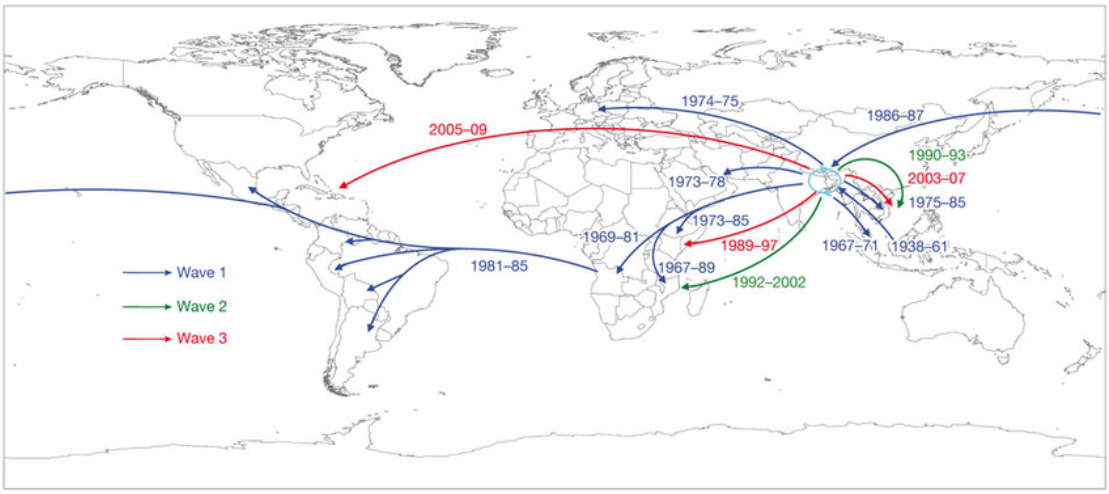

Figure 1.1: Transmission events inferred for the seventh-pandemic phylogenetic tree, drawn on a global map [75].

This can be linked to proliferation of the bacterium in water sources and changes in human behaviour, such as increased outdoor activities. Addressing the spread of cholera involves implementing comprehensive preventive measures. This includes improving access to clean water, promoting proper sanitation and hygiene practices, providing oral cholera vaccination in endemic areas and enhancing surveillance in conjunction with early response systems. Timely identification and treatment of cholera cases are critical. Public health interventions, such as health education, water purification efforts and infrastructure improvements play vital roles in reducing the incidence and impact of cholera.

1.2 Recent Cholera Outbreaks

Cholera was a major global problem in the 19^{th} century with large-scale epidemics in both Asia, Europe and Africa [104]. Although advances in medicine have reduced the impact of this scourge in developed countries, some regions have experienced serious cholera outbreaks in the recent past as highlighted in Table 1.2

The devasting effects of cholera epidemics, especially in developing countries, cannot be overemphasized. According to the World Health Organization (WHO), Africa continues to experience an exponential rise in cholera cases amid a global surge in the disease [90]. Scientific studies have

Table 1.2: Recent Outbreaks [81]

Years	Some of the Affected Regions	Approximate Deaths
1990s	Asia, Peru, DRC	30,000
2000s	Iraq, India, DRC	5,000
2010s	Nigeria, Haiti, Yemen	14,000
2020s	Niger	120

shown that Sub-Saharan Africa accounted for 60% of the global cholera burden estimates for the period 2008-2012 [3]. Between January 2022 and July 2023, a cumulative number of 217186, cases were reported to WHO Regional Office for Africa (AFRO), including 4002 deaths with CFR of 1.8% [80]. Outside Africa, Yemen accounted for 84% and 93% of global cholera cases in 2017 and 2019 respectively [47].

1.3 Cholera Background in Kenya

The first cholera cases were documented in Kenya in 1836, mostly along the coast where $20,000$ people died in Zanzibar alone [112]. The towns of Lamu, Malindi and Kilwa were almost completely depopulated [112]. There were no reported cases of cholera in Africa between 1870 and 1971 [112]. Since 1971, however, Kenya has experienced intermittent outbreaks which were more regular from 1974 as sketchily indicated in Table 1.3 [18, 112].

Table 1.3: Cholera cases in Kenya:$1974 - 2009$

PERIOD	CASES	DEATHS	COMMENTS
$1974 - 1989$			Average fatality of 3.57%
$1997 - 1999$	$33,400$		10% of all cholera cases reported in Africa
$2000 - 2006$	$1,157$		
By 2007 (cumulative to May 2007)	625	35	Fatality rate of 5.6%
By 2008 (cumulative to April)	$1,243$	67	Fatality rate of 5.39%
2009	$11,769$	274	Fatality rate of 2.33%

Table 1.3 shows that during the 3 years between 1997 and 1999, Kenya had 10% of all cases reported in Africa. From 2007-2009, reported cases increased significantly. Although fatality rates appear to have gone down from 5.6% to 2.3% during the same period, the economic constraints this trend puts on the government cannot be ignored. Kenya loses approximately US$ 270m annually due to poor sanitation [21]. One of the major causes of cholera in developing countries

like Kenya is poor sanitation and unhygienic living conditions [65]. Any ideas, proposals or recommendations that can minimize the impact of diseases like cholera in Kenya could be welcome. A researcher coming up with factual contributions could be helpful to society.

The outbreak under this study started around November 2014. Since that time, local newspapers highlighted fatalities arising from cholera from time to time. Hardly a day passed without a report on those who succumbed in different counties. The Daily Nation of 19^{th} May 2015 highlighted a schedule of known cholera deaths as at that date, as tabulated below:

Table 1.4: Reported cholera incidents between November 2014 and 19^{th} May 2015

COUNTY	**CASES**	**DEATHS**	Cumulative Fatality Rate (CMR)	**COMMENTS**
Nakuru	167	14	8.4	Active
Nairobi	239	12	5.0	Active
Migori	915	12	1.3	Controlled
Homa Bay	377	5	1.3	Controlled
Mombasa	81	5	6.2	Active
Muranga	471	3	0.6	Active
Bomet	272	2	0.7	Controlled
Baringo	8	0	0	Active
Kiambu	52	0	0	Active
Kirinyaga	150	0	0	Active
Total	2732	53	1.94	The average CMR is 1.94%

As seen from Table 1.4 above, cholera continued to cause more deaths in Kenya despite various interventions by the government. Within a period of about 6 months, 53 known deaths or a fatality rate of 1.94% had been recorded. Such an apparently low average CMR could be misleading on the impact of the disease. This does not openly reflect the emotional costs that accompany an epidemic of this nature. CMRs of 8.4% in active counties like Nakuru, 5% in Nairobi and 6.2% in Mombasa are a cause for concern. One could not tell what might have happened in the last 3 counties which had not reported any deaths by the time this study was undertaken. In fact, fatalities were reported from some counties after 1^{st} June 2015.

1.3.1 History of cholera modelling

The use of epidemic dynamics is an important approach to the method of studying the spread of infectious diseases [9, 40]. This approach is based on specific analysis of population growth,

spread of infectious diseases and related social factors [9]. Dynamic models for infectious diseases are mostly based on their compartmentalized structures which were firstly given by Kermack (1898-1976) and McKendrick (1876-1943) in 1927 but have been developed by many other bio-mathematicians since 1932 [9, 55].

In 2012, Hailegiorgis and Crooks demonstrated how cholera is spread in refugee camps [37]. Using the SEIR (Susceptible-Exposed-Infected-Recovered) model, they analysed how pollutants spread through floods passing the pathogen from infected to exposed individuals [37]. They concluded that through contaminated water sources, infected agents spread cholera bacteria radially throughout the system [37].

Following the above conclusion, Crooks and Hailegiorgis studied cholera dynamics in the same refugee camp in 2014. Their results were similar to their conclusion in 2012 [25]. Both findings highlighted the possibility of using agent-based models in the study of cholera dynamics [25].

From a Kenyan perspective so far, some researchers appear to have modelled cholera dynamics in closed populations in refugee camps. Models used did not emphasize government interventions in the fight against cholera spread [6, 25, 27, 36, 53, 61, 78].

By using mathematical models, researchers understand transmission dynamics of infectious diseases [109]. In the process, control programs are evaluated with a view to reducing both morbidity and mortality rates [109]. Compartmental models have been accepted as the most basic technique of modelling diseases [40]. In this method, the population is divided into different distinct groups [40].

There has been a growing concern over the effects of climatic changes and environmental deterioration [82]. Consequently, heightened interest in understanding how diseases' dynamics are subject to weather patterns is noticeable [82].

Water source contamination, rainfall and flooding have been associated with cholera outbreaks globally [96]. On the other hand, cholera dynamics cannot be delinked from interaction between the pathogen, humans and the environment [76, 107]. As a result, there exists two inescapable transmission pathways [76, 107]: human-to-human and environment-to-human. This is because cholera is caused by the bacterium *Vibrio cholerae*, is primarily spread through the ingestion of contaminated water or food. While human-to-human transmission can occur, it is relatively rare compared to other modes of transmission. This is because cholera bacteria must reach the

intestines to cause infection, and direct contact between individuals typically does not facilitate this [69]. The predominant mode of transmission is through the fecal-oral route, where bacteria from the feaces of an infected person contaminate water or food. This contaminated source is then ingested by another person, leading to infection. Therefore, the focus in cholera research and public health interventions is on improving water, sanitation, and hygiene (WASH) practices to prevent the contamination and spread of *Vibrio cholerae*. Given the low frequency of human-to-human retransmission, it is reasonable for research to prioritize other aspects of transmission dynamics [83]. Addressing environmental factors and ensuring safe water supplies are more impactful in controlling outbreaks and preventing the spread of the disease [99]. By focusing on these areas, research can more effectively contribute to reducing the incidence and impact of cholera. Therefore, human-to-human retransmission although important, is not frequent, thus it will be ignored in this research.

Studies have shown that the infection rate of cholera is a function of social and environmental factors [21]. It has also been noted that local environmental parameters are intensively associated with cholera dynamics [1]. It has been proved that *Vibrio cholerae* bacteria has a great capacity for environmental survival since it can live in water for many years [32]. Environmental factors in Kenya are significantly associated with increased cholera risks [96]. Other factors such as open defecation, lack of access to improved water sources and high levels of poverty are important contributors to cholera outbreaks. On average, 12% of Kenya's population practices open defecation and this figure is as high as 95% in some areas [23].

Complex cholera dynamics could be understood from different mathematical models which have addressed the problem [82]. Mathematical models of disease dynamics are central to a better understanding of responses to environmental forcing of disease dynamics [82]. When there is a cholera epidemic, there is a significant period of time during which some individuals may have been infected but are not yet infectious themselves [9, 72]. During this latent period, such individuals, who are referred to as asymptomatic, can transmit the disease [15]. Thus, unlike the SIR model, the SEIR model addresses the possibility of asymptomatic individuals transmitting cholera [25].

It has been shown that while symptomatic individuals may shed $10^9/ml$ of *V. cholerae* into the environment through faeces, those asymptomatic may only shed up to $10^5/ml$ per stool [25].

Since infective doses of environmental *V. cholerae* are suspected to be in the range 10^2 -10^6 cells, it is evident that depending on hyperinfectivity levels of the shed pathogen, asymptomatic individuals contribute significantly to the spread of cholera [42,51]. This is consistent with Haran's observation that an individual who feels perfectly healthy can be excreting amounts of pathogen large enough to transmit cholera [40].

The rest of this dissertation is organized as follows: Chapter 2 presents mathematical preliminaries, such as definition of theorems and basics used in the study. Chapter 3 analyses the basic model for cholera transmission dynamics and its mathematical analysis. Chapter 4 presents numerical solution to the system of equations describing the formulated cholera model. Chapter 5 presents an extended model to show improved sanitation's effect on reducing spread of the disease. Chapter 6 presents concluding remarks and recommendations.

Chapter 2

Literature Review

This chapter presents mathematical basics and literature review of well-known results and studies.

2.1 Mathematical Preliminaries and Definitions

Definition 2.1.1. *Lyapunov function is a non-negative function that decreases in time along the orbits of a dynamical system. It helps study the stability of equilibrium points [63].*

Definition 2.1.2. *We say that a non-singular $n \times n$ matrix A is Volterra-Lyapunov stable if there exists a positive diagonal $n \times n$ matrix M such that $MA + A^T M^T < 0$.*

Laws, principles, theorems/lemmas and equations

Definition 2.1.3. *Mass action law states that when substances A and B react with each other, the reaction rate is proportional to the concentration of A, denoted by $[A]$, and the concentration of B.*

Theorem 2.1. *[LaSalle's Invariance Principle] Suppose there is a neighbourhood D of O and continuously differentiable (time-independent) positive definite function $V : D \to \mathbb{R}$ whose orbital derivative $\dot{V}$ is negative semi-definite. Let I be the union of all complete orbits contained in $\{x \in D \mid \dot{V}(x) = 0\}$. Then there is a neighbourhood U of O such that for every $x_0 \in U, \omega(x_0) \subseteq I$ [63].*

Theorem 2.2. *[Pontryagin's Principle] Necessary conditions that (x^*, u^*) be an optimal solution for the optimal control problem are the existence of a non-zero k dimensional vector λ and an n-dimensional vector function $P(t)$ such that for $t \in [t_0, t_1]$:*

$$\dot{P(t)} = -P(t) f\left(t, x^*, u^*\right)$$

and

$$P(t) f(t, x, u) = H(t, x, u) = \max_{u \in U} \{H(t, x, u)\}.$$

Theorem 2.3. *[Next generation matrix method] In compartmental models for infectious disease transmission, individuals are categorized into several compartments: some are called disease compartments if the individuals therein are infected while others are called non-disease compartments. Suppose that there are $n > 0$ disease compartments and $m > 0$ non-disease compartments. Then a general compartmental disease transmission model can be written as*

$$X' = \mathcal{F}(x, y) - \mathcal{V}(x, y), \quad y' = g(x, y),$$

with $g = (g_1, \ldots, g_m)^T$. Here 1 denotes differentiation with respect to time ; $x = (x_1, \ldots, x_n)^T \in \mathbb{R}^{\mathrm{n}}$ and $y = (y_1, \ldots, y_m)^T \in \mathbb{R}^{\mathrm{m}}$ represent populations in disease compartments and non-disease compartments respectively; $F = (F_1, \ldots, F_n)^T$ and $V = (V_1, \ldots, V_n)^T$, where F_i represents the rate of new infections in the i^{th} disease compartment and V_i represents the transition terms, for example, death and recovery in the i^{th} disease compartment. Assume that $F_i(0, y) = 0, V_i(0, y) = 0, F_i(x, y) \geq 0, V_i(x, y) \leq 0$ whenever $x_i = 0$, and $\sum_{1=1}^{n} \mathcal{V}_i(x, y) \geq 0$ for all $x, y \geq 0, i = 1, \ldots, n$. Also assume that the disease-free system $y' = g(0, y)$ has a unique equilibrium $y = y_0 > 0$ that is locally asymptotically stable within the disease-free space. Define two $n \times n$ matrices

$$F = \left[\frac{\partial \mathcal{F}_i}{\partial x_j}\left(0, y_0\right)\right], \quad V = \left[\frac{\partial \mathcal{V}_i}{\partial x_j}\left(0, y_0\right)\right].$$

Assume that $F \geq 0$ and $V^{-1} \geq 0$, which are biologically reasonable. Then the next generation matrix is $K = FV^{-1}$ and the basic reproduction number $\mathcal{R}_0$ can be defined as the spectral radius of K, that is,

$$\mathcal{R}_0 = \rho\left(FV^{-1}\right).$$

Lemma 2.1.4. *Let* $D = \begin{bmatrix} d_{11} & d_{22} \\ d_{33} & d_{44} \end{bmatrix}$ *be a* 2×2 *matrix. Then* D *is Volterra-Lyapunov stable if and only if* $d_{11} < 0, d_{22} < 0$ *and* $\det(D) > 0$. *This indicates that all the equations are feasible in endemic equilibrium.*

2.2 Mathematical Modelling

Mathematical modelling of infectious diseases is the use of mathematical language to describe the process of transmission dynamics of a disease [102]. It is a tool that explores mathematical traceability of the transmission of a disease and helps in understanding spread dynamics of an epidemic [102]. Mathematical modelling in epidemiology, therefore, helps in understanding the underlying mechanisms that influence the spread of a disease and in the process, suggests control strategies [5].

2.2.1 History

Mathematical modelling in epidemiology is reported to have originated from Daniel Bernoulli when he solved a model for smallpox in 1760 [7]. Hamer analysed a discrete time model in 1906 and Ross developed differential equation models for Malaria in 1911 [31]. Soon afterwards, Ross won the second Nobel Peace Prize in medicine [13]. Kermack and McKendrick extended Ross models in 1926 and came up with the epidemic threshold results [13]. In essence, modern differential equation models of epidemics were introduced by Kermack and McKendrick but later expanded by Anderson and May [29]. In epidemiological terms, the threshold principle states that "if the average number of secondary infections caused by an average infective <1, a disease will die out but if this average >1, the disease will persist" [5]. Many researchers have referred to the average number of secondary infections as the basic reproduction number ($\mathbf{R_0}$) [52]. This is the most fundamental quantity used by epidemiologists [52]. Kermack and McKendrick have said that a single infective in an otherwise susceptible population will start an epidemic if the density

of susceptible exceeds a certain threshold [7]. Kermack and McKendrick have described $\mathbf{R_0}$ as the number of secondary cases generated from a single infective introduced into a susceptible population [7].

2.2.2 Mathematical Modelling of Cholera Epidemics

Different mathematical models have been proposed to investigate the complex epidemic and endemic behaviour of cholera [46]. In reality, mathematical models have been used to allow better understanding of cholera epidemiology retrospectively and to predict the impact of interventions in the future [35]. Thus, mathematical models have been used to synthesize knowledge of cholera into a quantitative framework [49].

Mathematical models play a great role in development of epidemiological theories [10]. They help to synthesize the current empirical knowledge about a disease, to infer cause-effect relationships and to suggest experimental designs to test alternative hypotheses [10]. Major studies of cholera begun in London when Dr. John Snow stopped a major cholera epidemic by closing a suspect water pump and in the process confirmed that cholera is a water-borne disease [100].

Several mathematical models of cholera transmission dynamics have been formulated and studied in response to Zimbabwe and Haiti epidemics, although only a small number of cholera transmission models have been developed [7, 100]. Notable among epidemiological studies is the Codeco model [21]. The model is popular for being the first to explicitly incorporate the environmental component to model a cholera epidemic [100]. The model, however, does not incorporate any control strategy [100]. In reality, once there is an epidemic, public enlightenment follows and control is inevitable [21]. This discovery paved way for further studies on cholera [21].

A basic and most fundamental control strategy for cholera is water treatment [84]. Capasso and Pareri-Fontana, to describe the dynamics of the 1973 epidemic of cholera in Italy, developed the first model [21]. This model was published in 1979, a period when mathematical modelling was in its infancy [84]. The model consisted of two coupled differential Equations (2.2.1) - (2.2.2) which describe dynamics of infected individuals in the community and dynamics of free-living bacteria population [10].

$$\begin{aligned} \frac{dx_1}{dt} &= -a_{11}x_1 + a_{12}x_2. \\ \frac{dx_1}{dt} &= g(x_1) - a_{22}x_2. \end{aligned} \tag{2.2.1}$$

The two state variables in this model include x_1 which describes concentration of the pathogen in an aquatic environment and x_2, the population of infected people [84]. In this model, all the constraints a_{ij} are constants [84]. The function of $g(x)$ accounts for the incidence of cholera infection [84]. Codeco thereafter developed a model with an additional equation for the susceptible individuals in the population [21]. He considered the population of susceptible individuals in a three compartmental model given by Eq. (2.2.2):-

$$\begin{aligned} \frac{dS}{dt} &= n\left(H - S\right) - a\lambda(B)S \\ \frac{dI}{dt} &= a\lambda\left(B\right)S - rI, \\ \frac{dB}{dt} &= eI - \left(mb - nb\right)B, \end{aligned} \tag{2.2.2}$$

where $\lambda\left(B\right) = \frac{B}{K+B}$.

In this model, S, I, B and H represent the susceptible population, infected individuals, concentration of the pathogen (*V. cholerae*) in the aquatic environment and the total population respectively [21]. n represents the human natural mortality rate $\left(day^{-1}\right)$ [84]. $\lambda\left(B\right)$is the probability of contact with *V. cholerae* and a is the rate of contact with untreated water [84].

Codeco was the first to build a cholera model that explicitly incorporates the environmental component, that is, the *V.cholerae* concentration in the water supply denoted by B, into a regular Susceptible-Infectious-Recovered (SIR) system to form a combined environment-to-human epidemiological model [21]. This model enables a careful study of the complex interaction between human host and environmental pathogen towards a better understanding of cholera transmission mechanisms and as such, it has motivated development of several other cholera models [100].

Building on Codeco's work, Hartley, Morris and Smith developed a more general model which took into account the different infective states of *V.cholerae*. The model consists of five equations which describe dynamics of a susceptible, infectious and removed human population and dynamics of hyper-infective and lower infective states [43]. The model incorporated the hyperinfective (HI) and non-hyperinfective (LI) states in transmission dynamics of the cholera pathogen [43]. This

model is indicated in Eq. (2.2.3):-

$$\begin{aligned}
\frac{dS}{dt} &= bN - \beta_L S\frac{B_L}{K_L+B_L} - \beta_H S\frac{B_H}{k_H+B_H} - bS,\\
\frac{dI}{dt} &= \beta_L S\frac{B_L}{k_L+B_L} + \beta_H S\frac{B_H}{k_H+B_H} - (\gamma+b)\,I,\\
\frac{dR}{dt} &= \gamma I - bR,\\
\frac{dB_H}{dt} &= \xi I - \chi B_H,\\
\frac{dB_L}{dt} &= \chi B_H - \delta_L B_L.
\end{aligned} \tag{2.2.3}$$

In this model B_H and B_L are concentrations of HI and LI per ml, I represents infectious individuals and S the susceptible population. β_L and β_H are the rates of ingestion of LI and HI *V. cholerae* respectively. In this model, the basic reproductive number was calculated and noted to be 18.2 when $\beta_H \backsim \beta_L$.

Mukandavire, Liao, Wang, Gaff, Smith and Morris built on the Codeco model by incorporating the human-to-human factor. They estimated the basic reproduction number (R_0) for the 2008 to 2009 cholera outbreaks in Zimbabwe [73]. They presented a model fitted to the Zimbabwean data that provides insights into the nature of the epidemic in Zimbabwe and, on a broader scale, to control of cholera at a global level [100]. More specifically, they used Zimbabwean data to derive estimates of the basic reproductive number (R_0) of cholera on a regional basis [113]. The model is represented by the system in Eq. (2.2.4) below:-

$$\begin{aligned}
\frac{dS}{dt} &= \mu N - \beta_e S\frac{B}{k+B} - \beta_h SI - \mu S,\\
\frac{dI}{dt} &= \beta_e S\frac{B}{k+B} + \beta_h SI - (\gamma+\mu)\,I,\\
\frac{dR}{dt} &= \gamma I - \mu R,\\
\frac{dB}{dt} &= \xi I - \delta B.
\end{aligned} \tag{2.2.4}$$

Ashleigh, Tien, Eisenberg, David, J., Junling and David, N. built a SIR compartmental transmission model that characterized the population as susceptible to infection, infected and infectious to others. Recovered or otherwise were removed from risk to further infection [103]. They assumed that cholera could be transmitted through either contaminated water or close contact with infectives but that water borne transmission was a far more important method of transmission. They added a water compartment to the model [100].

2.3 Epidemiological Models

A model is an object or a concept that is used to represent something else in a form we can comprehend [14]. A mathematical model is an explicit mathematical description of the simplified dynamics of a system [7]. Thus, a model is often an approximation of conceptual experiments which would otherwise be difficult or impossible to do [7]. Basic mathematical models of infectious diseases' transmission describe transitions of individuals between susceptible, infectious and recovered states

Models on behaviour of infectious diseases in large populations often consider each individual as being in a particular state [19]. These states are often referred to as compartments and the corresponding models are called compartmental models [19]. This has made the use of compartmental models handy because of the need to use models based on continuous variables [66]. A compartmental model, therefore, provides a framework for the study of a dynamical system such as disease dynamics in a large population [71]. A compartmental model may also be defined as a mathematical representation of a body created to study a mixer of objects in a dynamical system [19].

Most mathematical models on cholera make use of compartmental models which describe the basic features of disease transmission [49]. Mathematical models of interest in cholera modelling make use of basic concepts in Ordinary Differential Equations (ODEs) [10]. These concepts make understanding of fundamental mechanisms of disease transmission easy to follow for effective prevention and interventional strategies against outbreaks [101]. Consequently, the progress of an epidemic through the population is highly tractable to mathematical modelling [54]. In particular, the first attempt to model and hence predict or explain spread patterns dates back over 100 years although it was the work of Kermack and McKendrick that established the basic foundations of the subject [54], [39], [55]. These early models, and many subsequent revisions and improvements operated on the principle that individuals can be classified by their epidemiological status i.e. susceptible to the infection, infected and therefore infectious and recovered and are therefore no longer infectious [100].

2.3.1 The SIS model

The simplest compartment model often assumes a person can be in any one of the two states, i.e. either susceptible (S) or infectious (I) [33]. These two state possibilities define the SIS model [33]. In this model, an individual never enters "recovered" state, but alternates between infected and susceptible as indicated in Figure 2.1 [33].

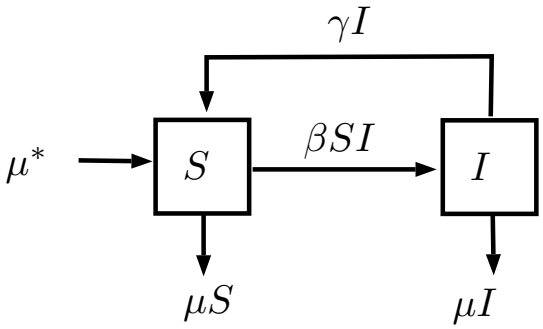

Figure 2.1: Diagram of SIS compartment model showing the transmission rate, β, the death rate, μ, the birth rate μ^* and the recovery rate γ.

In SIS model, individuals move from the Susceptible state (S) to the Infectious state (I) by interacting with infectious individuals [33]. The model assumes no immunity against a given disease [106]. The rate of infection depends on the contact between Susceptible and Infected (SI), while recovery is also at a constant rate proportional to the number of infected (b). The corresponding equations for the model are:-

$$\begin{aligned} \frac{dS}{dt} &= bI - aSI, \\ \frac{dI}{dt} &= aSI - bI, \end{aligned} \tag{2.3.1}$$

where a and b are the infection and recovery rates respectively [52].

2.3.2 The SIR model

In this model, an individual occupies any of the three compartments, that is, Susceptible, Infective or Recovered [102]. Other mathematical models such as Susceptible, Infectious, Recovered and Susceptible (SIRS) and Susceptible, Exposed, Infectious and Recovered (SEIR), are modifications of the SIR model [113], [52]. For instance, sometimes this model may include a class of exposed

individuals, E, that is, those who are infected but are not infectious, and that becomes the SEIR model [33]. On the other hand, an extension of the SIR model is the SIRS model, which is a model used to describe endemic infection [33]. The SIR model is one of the earliest mathematical models that were developed by Kermack and McKendrick in 1927 [52]. Besides, the SIR model is one of the simplest and most fundamental of all epidemiological models [33]. It is based on calculating the proportion of population in each of the three classes, that is, susceptible, infected and recovered, and determining the rates of transition between these classes [33]. The SIR model is used in epidemiology to compute the number of susceptible, infected and recovered individuals in a population during a time-period (t) under certain conditions [29]. It mainly describes diseases which confer immunity against reinfection [106]. The diagram of SIR model is shown in Figure 2.2.

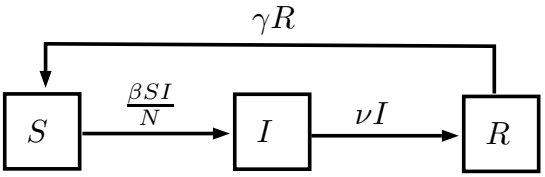

Figure 2.2: Diagram of the SIR model [102].

The SIR model is represented by the following system of differential equations [29];

$$\begin{aligned} \frac{dS}{dt} &= -\frac{\beta SI}{N} + \gamma R, \\ \frac{dI}{dt} &= \frac{\beta SI}{N} - \nu I, \\ \frac{dR}{dt} &= \nu I - \gamma R. \end{aligned}$$

Mathematical modelling provides a unique approach to gain basic knowledge in transmission dynamics [100]. The model formulation process clarifies assumptions, variables and parameters [50]. Mathematical models provide results such as thresholds, basic reproduction numbers, contact numbers and replacement numbers [50].

Mathematical modelling of disease transmission often uses a trade-off between simple models, which omit most details and are designed only to highlight general qualitative behaviour, and detailed models, usually designed for specific reasons for short-term and long-term prediction [35]. Detailed models are generally difficult or impossible to solve analytically and hence their usefulness

for theoretical purposes is limited, although their strategic value may be high [106]. Consequently, many researchers use simple models since they constitute the building blocks for other models which include structures that are more detailed [106].

To effectively stop the spread of infectious diseases among the population, many governments have resorted to immunization and vaccinations [102]. When a large number of the population has been vaccinated and are therefore immune to such diseases, there is a likelihood that very low number is susceptible to infection [50]. This is known as herd immunity, which can be used to describe the proportion of those who may be described as free from being infected among individuals in a population [100]. Therefore, a population is said to have herd immunity from a disease if enough people are immune such that the disease would not spread if it were suddenly introduced anywhere in the population [52]. The theory of herd immunity claims that diseases are passed from person-to-person and it is difficult to maintain a chain of infection when a large number of the population is immune [50]. This can be calculated as herd immunity threshold, H_t [110]. Thus, herd immunity threshold is the percentage of the population that needs to be immune to control transmission of a disease [52].

It can be seen that

$$H_t = \frac{R_0 - 1}{R_0}, \tag{2.3.2}$$

where R_0 is the basic reproduction number [52]. The basic reproduction number (R_0) referred to earlier is the central concept of mathematical epidemiology [19]. R_0 gives average number of secondary infections that result from the introduction of a single infective individual into an entirely susceptible population [19], [29], [113]. R_0 tells us how easy or difficult it is to eradicate an infection in a population [17]. If $R_0 > 1$, this means that a disease either has invaded the population or is persistent in that population [19].

Mathematical models play a great role in development of epidemiological theories [10]. Models of disease transmission provide guidance in making logistical and interventional policy decisions during epidemics [113]. Different models have been formulated to address disease spread in different locations [113]. Some models are said to be simple models while others have been described as too complex [113].

2.4 Cholera Treatment and Vaccinations

Cholera treatment entails a wide range of approaches. For instance, rehydration therapy, which is the cornerstone of cholera treatment, involves replacing fluids and electrolytes lost through severe diarrhoea and vomiting [57]. Oral rehydration solutions (ORS) are commonly used, providing a balanced mix of salts, sugars and water to restore hydration and electrolyte balance. In severe cases where dehydration is profound, intravenous fluids may be administered to rapidly replenish what is lost [64]. Swift and appropriate fluid replacement can significantly reduce the levels of mortality associated with cholera.

Antibiotics can help shorten the duration and reduce severity of cholera symptoms [67]. Commonly used antibiotics include doxycycline, azithromycin and ciprofloxacin. Antibiotics are particularly important in reducing the duration of shedding of Vibrio cholerae bacteria, thereby decreasing the risk of further transmission [108]. Zinc supplements may be beneficial, especially in children, as they help reduce severity and duration of diarrhoea [108].

International Public Health authorities in collaboration with the Center for Disease Control and Prevention (CDC) and the World Health Organization (WHO) have come up with the Global Task Force on Cholera Control (GTFCC) objectively to reduce cholera deaths by 90% before 2030 [20]. Effective combating of cholera outbreaks involves harnessing the power of oral cholera vaccines [70]. Dukoral, Shanchol and Euvichol are among WHO-prequalified options which exemplify the success of preventive measures [70]. Administered orally, these vaccines bestow immunity against Vibrio cholerae, presenting a crucial front-line defence. Strategic and widespread vaccination campaigns constitute a proactive stance against cholera. Targeting high-risk areas and populations especially those dwelling in crowded or unsanitary conditions creates a formidable barrier which curb the potential spread [93] of cholera. Recommendation of pre-exposure and post-exposure prophylaxis with oral cholera vaccines is a dynamic strategy in response to outbreaks. Swift action provides short-term protection, bolstering a collective defence against the disease. Elevating the standards of water and sanitation infrastructure is pivotal for a sustained defence against cholera transmission [30]. Access to clean water and improved sanitation facilities form a backbone of preventive measures within the environment. Empowering communities with the knowledge of proper hygiene practices is fundamental. This grassroot

approach minimizes the risk of contamination, fostering a culture of health-conscious behaviours that actively contribute to cholera prevention.

Chapter 3

MATHEMATICAL ANALYSIS OF THE MODEL

3.1 Model formulation

After evaluating different epidemic models, it was considered that for the purposes of this research, the most suitable model was a modification of SIR. That modification included addition of vaccinated compartment and splitting of the infectious compartment to cover both infectious asymptomatic and symptomatic compartments. In the model, it is assumed that intervention by vaccination takes place. Human population is subdivided into six categories, namely, Susceptible (S), Vaccinated (V), Infectious but asymptomatic (I_a), Infectious with symptoms (I_s), Treated (T) and Recovered (R). An open population is assumed with a total population N at time t represented in these categories as:

$$N = S + I_a + I_s + V + T + R. \tag{3.1.1}$$

Susceptible individuals, S, are increased by recruitment at rate Λ and by those waned but vaccinated at rate ωV. However, susceptible individuals are also reduced by vaccination at rate ρ,

asymptomatic infectious at rate $f\lambda$, symptomatic infectious at rate $(1-f)\lambda$ and natural deaths at rate μS. Similarly, population of vaccinated individuals, V, is increased by vaccination at rate ρS, reduced by those waned but vaccinated at rate ω and by natural deaths at rate μ. Population of asymptomatic-infectious individuals, I_a, is generated by progression of susceptible individuals' movement to asymptomatic-infectious state after contact with pathogen at rate $f\lambda S$. Population of asymptomatic-infectious individuals is diminished by those recovering at rate θ_a and natural deaths at rate μ.

Likewise, population of symptomatic individuals is generated by progression of susceptible individuals to symptomatic-infectious state after contact with pathogen at rate $\lambda(1-f)S$. It is reduced by recovery of symptomatic-infectious individuals at rate θ_s, by treated individuals at rate τ and by natural deaths at rate μ. Population of treated individuals is generated at rate τI_s, reduced at natural death rate at which humans die, μ and by those recovering at rate θ_t. Unlike I_s and I_a, treated individuals do not contribute to infections. Population of recovered individuals, R, is generated at rates $\theta_a I_a$, $\theta_s I_s$ and $\theta_t T$ and reduces at death rate μ. *Vibrio cholerae* concentration, B, is generated within the environment following shedding of the pathogen by infectious individuals with or without cholera symptoms. This concentration is also increased by infectious asymptomatic at rate φ_a and by infectious symptomatic individuals at rate φ_s. At the same time, pathogen population is decreased by natural loss of *V. cholerae* in the environment at rate μ_B.

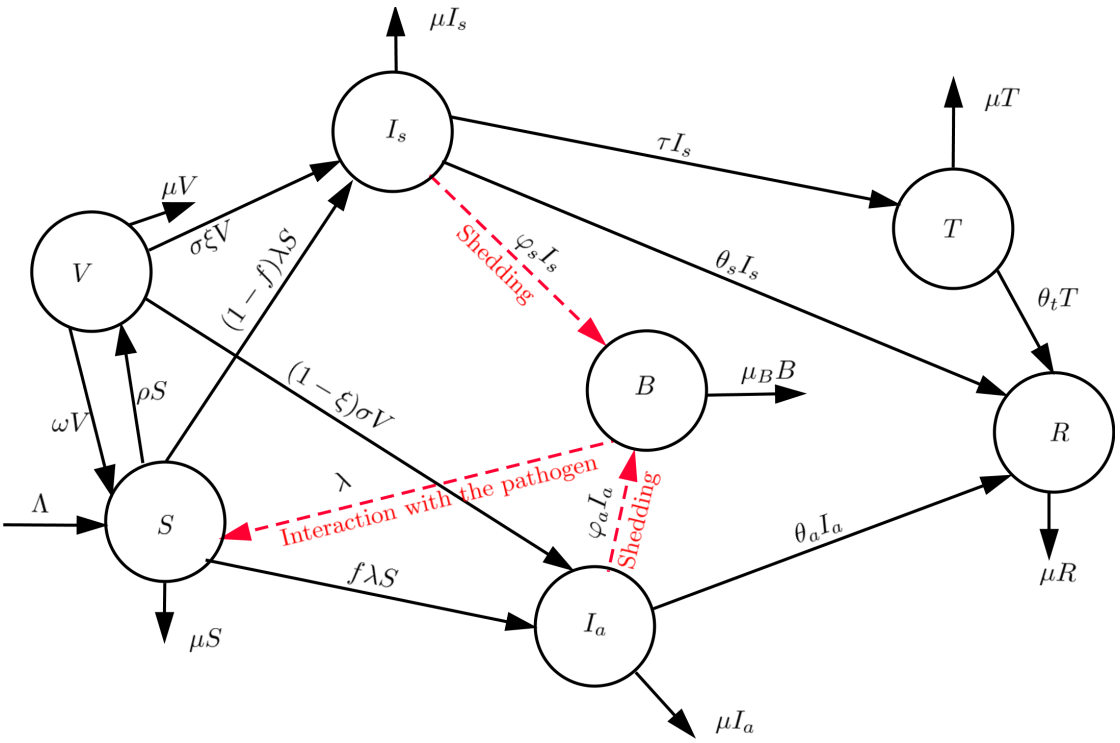

Figure 3.1: Model flow chart where the population is divided into Susceptible, Vaccinated, Infectious Asymptomatic, Infectious Symptomatic, Treated, Recovered and *Vibrio Cholerae* population. The flow chart is summarized in Equations (3.1.2)-(3.1.8).

The following Ordinary Differential Equations are derived to describe cholera dynamics as depicted in Figure 3.1:

$$\frac{dS}{dt} = \Lambda + \omega V - (\rho + \mu + \lambda)S \tag{3.1.2}$$

$$\frac{dV}{dt} = \rho S - (\omega + \mu + \sigma)V \tag{3.1.3}$$

$$\frac{dI_s}{dt} = \sigma\xi V + (1-f)\lambda S - (\theta_s + \tau + \mu)I_s \tag{3.1.4}$$

$$\frac{dI_a}{dt} = (1-\xi)\sigma V + f\lambda S - (\theta_a + \mu)I_a \tag{3.1.5}$$

$$\frac{dT}{dt} = \tau I_s - (\mu + \theta_t)T \tag{3.1.6}$$

$$\frac{dR}{dt} = \theta_t T + \theta_a I_a + \theta_s I_s - \mu R \tag{3.1.7}$$

$$\frac{dB}{dt} = \varphi_a I_a + \varphi_s I_s - \mu_B B \tag{3.1.8}$$

where $\lambda = \beta \frac{B}{K_B + B}$. The total population N at time t is represented as

$$N = S + I_s + I_a + V + T + R. \tag{3.1.9}$$

It is assumed that all parameters are positive and their corresponding initial conditions are

$$\begin{aligned} &N(0) = N_0, S(0) = S_0 > 0, \quad V(0) = V_0 \geq 0, \\ &I_s(0) = I_{s0} \geq 0, \qquad\qquad I_a(0) = I_{a0} \geq 0, \\ &T(0) = T_0 \geq 0, \qquad\qquad R(0) = R_0 \geq 0, B(0) = B_0 > 0. \end{aligned} \tag{3.1.10}$$

Table 3.1 presents model parameters.

Table 3.1: Parameter Descriptions

Parameter	**Description**
Λ	Recruitment Rate
f	Progressive rate of susceptible individuals movement to asymptomatic-infectious state
λ	Contact rate
K_B	Concentration of *V. cholerae* that yields 50% chance of infection
σ	Efficacy of vaccine dose
θ_a	Recovery rate of asymptomatic-infectious individuals
θ_t	Recovery rate of treated individuals
ω	Waning rate of vaccine
ρ	Vaccination rate
ξ	Fraction of vaccinated individuals who become symptomatic-infectious individuals
θ_s	Recovery rate of symptomatic-infectious individuals
τ	Treatment rate for symptomatic-infectious individuals
μ_B	Rate of natural loss of *Vibrio cholerae*
φ_a	Contribution of asymptomatic-infectious individuals to the *Vibrio cholerae* concentration
φ_s	Contribution of symptomatic-infectious individuals to the *Vibrio cholerae* concentration
β	Ingestion rate of *Vibrio cholerae* by humans due to contact with contaminated sources
μ	Natural death rate of humans

3.2 Well-posedness of the system

Theorem 3.1. *The model described by the system represented by Equations* (3.1.2)-(3.1.8) *has a unique solution* X *which is positive and bounded if* $\urcorner$ *in Eq.* (3.2.1) *is given by Eq.* (3.2.9) *whenever the initial conditions* $X(0) = (S_0, V_0, I_{s_0}, I_{a_0}, T_0, R_0, B_0)$ *are non-negative.*

Proof. Let $X_1 = (S, V, I_s, I_a, T, R)\,, X_2 = B$

$$\begin{aligned} \urcorner : \Omega_7 &\to \mathbb{R}_+^7 \\ X &\to X^{'}. \end{aligned} \tag{3.2.1}$$

Let $\Omega = \left\{ X = (S, V, I_s, I_a, T, R, B) \in \mathbb{R}_+^7 : S + V + I_s + I_a + T + R \leq N \ \ : B \leq \frac{(\varphi_a + \varphi_b)N}{\mu_B} \right\}$

$$\urcorner_1(X) = \frac{dS}{dt} = \Lambda + \omega V - (\rho + \mu + \lambda)S \tag{3.2.2}$$

$$\urcorner_2(X) = \frac{dV}{dt} = \rho S - (\omega + \mu + \sigma)V \tag{3.2.3}$$

$$\urcorner_3(X) = \frac{dI_s}{dt} = \sigma\xi V + (1 - f)\lambda S - (\theta_s + \tau + \mu)I_s \tag{3.2.4}$$

$$\urcorner_4(X) = \frac{dI_a}{dt} = (1 - \xi)\sigma V + f\lambda S - (\theta_a + \mu)I_a \tag{3.2.5}$$

$$\urcorner_5(X) = \frac{dT}{dt} = \tau I_s - (\mu + \theta_t)T \tag{3.2.6}$$

$$\urcorner_6(X) = \frac{dR}{dt} = \theta_t T + \theta_a I_a + \theta_s I_s - \mu R \tag{3.2.7}$$

$$\urcorner_7(X) = \frac{dB}{dt} = \varphi_a I_a + \varphi_s I_s - \mu_B B. \tag{3.2.8}$$

Thus, Equations (3.2.2)-(3.2.8) can be written as

$$X^{'} = \urcorner(X); X(0) = (S_0, V_0, I_{s_0}, I_{a_0}, T_0, R_0, B_0) \in \Omega. \tag{3.2.9}$$

The system of Equations (3.1.2)-(3.1.8) is supplemented by the initial conditions in Eq. (3.2.9) with initial conditions can be expressed as: $\frac{dX}{dt} = \urcorner(X), X(0) = X_0$, where $X = (S, V, I_s, I_a, T, R, B)$ is a vector in $\mathbb{R}^7$ and $f(X) = \left(\urcorner_1(X), \urcorner_2(X), \urcorner_3(X), \urcorner_4(X), \urcorner_5(X), \urcorner_6(X), \urcorner_7(X) \right)^T$ is a vector field in $\mathbb{R}^7$ such that $\urcorner_1(X) - \urcorner_7(X)$ are defined by Equations (3.2.2)-(3.2.8) respectively.
It is easy, using the standard dynamical system in Theorem 2.1.3 [97, p. 102] to see that f is differentiable, hence, locally Lipschitz, thus there exists a unique local solution of Equations (3.1.2)-(3.1.8). If $X(0) = (S_0, V_0, I_{s_0}, I_{a_0}, T_0, R_0, B_0) \geq 0$, from Equations (3.1.2)-(3.1.8), we have $S^{'}(t) = \Lambda + \omega V \geq 0$, whenever $S = 0$, $V^{'} = \rho S \geq 0$, whenever $V = 0$, $I_s^{'} = \sigma\xi V + (1 - f)\lambda S \geq 0$, whenever $I_s = 0$, $I_a^{'} = (1 - \xi)\sigma V + f\lambda S \geq 0$, whenever $I_a = 0$, $T^{'} = \tau I_s \geq 0$, whenever $T = 0$,

$R^{'} = \theta_t T + \theta_a I_a + \theta_s I_s \geq 0$, whenever $R = 0$ and $B^{'} = \varphi_a I_a + \varphi_s I_s \geq 0$, whenever $B = 0$.

Using Proposition $B.7$ of [94], the solution of the system of Equations (3.1.2)-(3.1.8) is non-negative for all $t > 0$.

We can now verify that the dissipation condition is as follows:

$$\begin{aligned}
\urcorner_F(X).X &= (\urcorner_1, \urcorner_2, \urcorner_3, \urcorner_4, \urcorner_5, \urcorner_6, \urcorner_7).(S, V, I_s, I_a, T, R, B) \\
&= \urcorner_1 S + \urcorner_2 V + \urcorner_3 I_s + \urcorner_4 I_a + \urcorner_5 T + \urcorner_6 R + \urcorner_7 B \\
&= (\Lambda + \omega V - m_1 S)\, S + (\rho S - m_2 V)\, V \\
&+ (\sigma \xi V + (1-f)\lambda S - m_3 I_s)\, I_s \\
&+ ((1-\xi)\sigma V + f\lambda S - m_4 I_a)\, I_a \\
&+ (\tau I_s - m_5 T)\, T + (\theta_t T + \theta_a I_a + \theta_s I_s - \mu R)\, R + (\varphi_a I_a + \varphi_s I_s - \mu_B B)\, B \\
&= (m_1 + m_2 + m_3 + m_4 + m_5)(S^2 + V^2 + I_s^2 + I_a^2 + T^2 + R^2 + B^2) + \Lambda S + \omega V S \\
&+ \rho S V + \delta \xi V I_s + (1-f)\lambda S I_s + (1-\xi)\sigma V I_a \\
&+ f\lambda S I_a + \tau I_s T + \theta_t T R + \varphi_a I_a B + \varphi_s I_s B \\
&\leq a|X|^2 + q
\end{aligned} \tag{3.2.10}$$

where $a = (m_1 + m_2 + m_3 + m_4 + m_5)$ and $q = aN^2$ representing constants whose magnitudes are positive and $m_1 = \rho + \mu + \lambda, m_2 = \omega + \mu + \sigma, m_3 = \theta_s + \tau + \mu, m_4 = \theta_a + \mu$ and $m_5 = \mu + \theta_t$. Therefore, $X(t)$ of the system of Equations (3.1.2)-(3.1.7) is well defined in time. Hence, $S(t) \leq N, V(t) \leq N, I_s(t) \leq N, I_a(t) \leq N, T(t) \leq N, R(t) \leq N, B(t) \leq B; \forall t \geq 0$. Thus, X is bounded.

□

3.3 Disease Free Equilibrium

The system of Equations (3.1.2)-(3.1.8) has a disease free equilibrium. At Disease Free Equilibrium (DFE), we have points

$$\frac{dS}{dt} = \frac{dV}{dt} = \frac{dI_s}{dt} = \frac{dI_a}{dt} = \frac{dT}{dt} = \frac{dR}{dt} = \frac{dB}{dt} = 0. \tag{3.3.1}$$

From Eq. (3.1.3),

$$S_0 = \frac{m_2 V_0}{\rho}. \tag{3.3.2}$$

Eq. (3.3.2) is put into Eq. (3.1.2) with the left hand side equal to 0 to obtain

$$\Lambda + \omega V_0 - m_1 \frac{m_2 V_0}{\rho} = 0, \tag{3.3.3}$$

$$\text{from where } V_0 = \left(\frac{\Lambda \rho}{m_1 m_2 - \omega \rho} \right) \text{ for } m_1 m_2 \geq \omega \rho, \tag{3.3.4}$$

$$\text{and } S_0 = \frac{m_2 \Lambda}{m_1 m_2 - \omega \rho}. \tag{3.3.5}$$

Substitute Eq. (3.3.5) and Eq. (3.3.4) into Eq. (3.1.4) to obtain

$$I_{s_0} = \frac{(f-1)\lambda \Lambda m_2}{m_3(\omega \rho - m_1 m_2)}. \tag{3.3.6}$$

Subsequently, Eq. (3.1.5) is used to obtain

$$I_{a_0} = \frac{f \lambda \Lambda m_2}{m_4(m_1 m_2 - \omega \rho)}. \tag{3.3.7}$$

Using algebraic manipulations, S_0 and V_0 values are substituted into Eq. (3.1.4) to obtain

$$\frac{\sigma \xi m_3 \rho I_{s_0}}{(1-f)\lambda m_2} + \frac{(1-f)\lambda m_3 I_{s_0}}{(1-f)\lambda} - m_3 I_{s_0} = 0. \tag{3.3.8a}$$

Eq. (3.3.8a) is then simplified to get

$$\frac{\sigma \xi m_3 \rho I_{s_0}}{(1-f)\lambda m_2} = 0, \tag{3.3.8b}$$

$$\text{but } \frac{\sigma \xi m_3 \rho}{(1-f)\lambda m_2} \neq 0, \implies I_{s_0} = 0. \tag{3.3.8c}$$

At the same time,

$$\frac{(1-\xi)\sigma m_4 \rho I_{a_0}}{f\lambda m_2} + \frac{f\lambda m_4 \mu I_{a_0}}{f\lambda\mu} - m_4 I_{s_0} = 0 \tag{3.3.9a}$$

$$\frac{(1-\xi)\sigma m_4 \rho I_{a_0}}{f m_2} = 0 \tag{3.3.9b}$$

$$\text{but } \frac{(1-\xi)\sigma m_4 \rho}{f m_2} \neq 0, \implies I_{a_0} = 0. \tag{3.3.9c}$$

Since $I_{s_0} = I_{a_0} = 0$ (see Eq. (3.3.8c) and Eq. (3.3.9c)) and substituting this into Equations (3.1.6)-(3.1.8) gives $T_0 = R_0 = B_0 = 0$.

Therefore, $X_0 = (S_0, V_0, I_{s_0}, I_{a_0}, T_0, R_0, B_0) = \left(\left(\frac{m_2\Lambda}{m_1 m_2 - \omega\rho}\right), \left(\frac{\Lambda\rho}{m_1 m_2 - \omega\rho}\right), 0, 0, 0, 0, 0\right)$ is the DFE point where $m_1 = (\rho + \mu + \lambda), m_2 = (\omega + \mu + \sigma), m_3 = (\theta_s + \tau + \mu), m_4 = (\theta_a + \mu)$ and $m_5 = (\mu + \theta_t)$.

3.3.1 The Control Reproduction Number

$\mathcal{R}_0$ is the average number of secondary infections produced by a single infected individual in a completely susceptible population, where there are no interventions in place [105]. $\mathcal{R}_C$ is the average number of secondary infections produced by a single infected individual in a population where control measures are implemented [44]. The next generation matrix method described in [4, 105] is used to rewrite the main system in the following form:

$$\begin{aligned} \dot{x_i} &= \mathcal{F}(x, y) - \mathcal{V}_{\mathbf{\Gamma}i}(x, y) \\ \dot{y_j} &= g(x, y) \end{aligned} \tag{3.3.10}$$

with

$$\begin{aligned} x &= (I_s, I_a, T, B)^\top \\ y &= (S, V, R)^\top. \end{aligned}$$

Let $F = \nabla\mathcal{F}|_{(S^*, V^*, 0)}$ and $\Gamma = \nabla\mathcal{V}_{\mathbf{\Gamma}}|_{(S^*, V^*, 0)}$ be the Jacobian matrices of maps $\mathcal{F}$ and $\mathcal{V}_{\mathbf{\Gamma}}$ evaluated at the DFE.

$$\mathcal{F} = \begin{pmatrix} (1-f)\lambda S \\ f\lambda S \\ 0 \\ 0 \end{pmatrix}, \mathcal{V}_{\mathbf{\Gamma}} = \mathcal{V}_{\mathbf{\Gamma}}{}^{-} - \mathcal{V}_{\mathbf{\Gamma}}{}^{+} = \begin{pmatrix} m_3 I_s - \sigma\xi V \\ m_4 I_a - (1-\xi)\sigma V \\ m_5 T - \tau I_s \\ \mu_B B - \varphi_s I_s - \varphi_a I_a \end{pmatrix}.$$

Vector $\mathcal{F}$ represents the rate of new infections in compartment i, vector $\mathcal{V}_{\mathbf{\Gamma}}{}^{+}$ represents the rate of new infections in compartment i by other means and vector $\mathcal{V}_{\mathbf{\Gamma}}{}^{-}$ is the rate of transfer of individuals out of compartment i. Jacobian matrices for $\mathcal{F}$ and $\mathcal{V}_{\mathbf{\Gamma}}$ at disease free equilibrium are given by matrices F and $\mathcal{V}_{\Gamma}$ respectively and are defined as follows:

$$F = \frac{\partial \mathcal{F}}{\partial X}$$

and

$$\mathcal{V}_{\Gamma} = \frac{\partial \mathcal{V}_{\mathbf{\Gamma}}}{\partial X}.$$

Therefore, there is F and its corresponding value at DFE, where $S_0 = \left(\frac{m_2\Lambda}{m_1 m_2 - \omega\rho}\right)$, $V_0 = \left(\frac{\Lambda\rho}{m_1 m_2 - \omega\rho}\right)$ and $B_0 = 0$ is given by

$$F = \begin{pmatrix} 0 & 0 & 0 & \frac{B_0 S_0 \beta(f-1)}{(B_0+K_B)^2} - \frac{S_0\beta(f-1)}{B_0+K_B} \\ 0 & 0 & 0 & \frac{S_0\beta f}{B_0+K_B} - \frac{B_0 S_0 \beta f}{B_0+K_B^2} \\ 0 & 0 & 0 & 0 \\ 0 & 0 & 0 & 0 \end{pmatrix} = \begin{pmatrix} 0 & 0 & \frac{\beta m_2 \Lambda(f-1)}{K_B(\omega\rho - m_1 m_2)} \\ 0 & 0 & \frac{\beta f m_2 \Lambda}{K_B(m_1 m_2 - \omega\rho)} \\ 0 & 0 & 0 \end{pmatrix},$$

$$\mathcal{V}_{\Gamma} = \begin{pmatrix} m_3 & 0 & 0 & 0 \\ 0 & m_4 & 0 & 0 \\ -\tau & 0 & m_5 & 0 \\ -\varphi_s & -\varphi_a & 0 & \mu_B \end{pmatrix},$$

and the inverse of $\mathcal{V}_{\Gamma}$ gives

$$\mathcal{V}_{\Gamma}^{-1} = \begin{pmatrix} \frac{1}{m_3} & 0 & 0 & 0 \\ 0 & \frac{1}{m_4} & 0 & 0 \\ \frac{\tau}{m_3 m_5} & 0 & \frac{1}{m_5} & 0 \\ \frac{\varphi_s}{m_3 \mu_B} & \frac{\varphi_a}{m_4 \mu_B} & 0 & \frac{1}{\mu_B} \end{pmatrix},$$

where $m_1 = (\rho + \mu + \lambda), m_2 = (\omega + \mu + \sigma), m_3 = (\theta_s + \tau + \mu), m_4 = (\theta_a + \mu)$ and $m_5 = (\mu + \theta_t)$. The next generation matrix of the system of the model is given by $F\mathcal{V}_{\Gamma}^{-1}$. The control reproduction number is given by the spectral radius of $F\mathcal{V}_{\Gamma}^{-1}$, meaning $F\mathcal{V}_{\Gamma}^{-1} = \mathcal{R}_C$ or the largest eigenvalues of $F\mathcal{V}_{\Gamma}^{-1}$. Thus,

$$\begin{aligned} \mathcal{R}_C &= \tfrac{\Lambda\beta m_2(m_4\varphi_s + f m_3\varphi_a - f m_4\varphi_s)}{K_B m_3 m_4 \mu_B (m_1 m_2 - \omega\rho)}, \\ &= \tfrac{\beta m_2 \Lambda(m_4\varphi_s(1-f) + f m_3\varphi_a)}{K_B m_3 m_4 \mu_B (m_1 m_2 - \omega\rho)}, \\ &= \tfrac{1}{K_B \mu_B (m_1 m_2 - \omega\rho)} \left(\tfrac{\beta m_2 \Lambda \varphi_s (1-f)}{m_3} + \tfrac{f\varphi_a}{m_4} \right). \end{aligned} \tag{3.3.11}$$

3.3.2 Stability Analysis

Local stability analysis of DFE

Theorem 3.2. *The DFE,* $X_0 = \left(\frac{m_2\Lambda}{m_1 m_2 - \omega\rho}, \frac{\Lambda\rho}{m_1 m_2 - \omega\rho}, 0, 0, 0, 0, 0 \right)$ *for the system of Equations* (3.1.2)-(3.1.8)*,* X_0 *is locally asymptotically stable if* $\mathcal{R}_C < 1$ *and unstable if* $\mathcal{R}_C > 1$ *where* $\mathcal{R}_C$ *is defined by Eq.* (3.3.11)*.*

Proof. See proof of Theorem 2.1 in [105]. □

Global stability analysis of DFE

Theorem 3.3. *If* $\mathcal{R}_C \leq 1$*, then the DFE of the system of Equations* (3.1.2)-(3.1.8) *is globally asymptotically stable in* $\Omega = \{X = (S, V, I_s, I_a, T, R, B) \in \mathbb{R}^7 : S + V + I_s + I_a + T + R \leq N$ *and* $B \leq \frac{(\varphi_a + \varphi_b)N}{\mu_B}\}$ *and is unstable if* $\mathcal{R}_C > 1$*.*

Proof. The matrix-theoretic method as described in Theorem 2.1 in [92] is used. Let $x = (I_s, I_a, T, B)^T$ and $y = (S, V, R)$. F, V_{Γ}, $\mathcal{F}$ and $\mathcal{V}$ are considered as defined in Section 3.3.1. If the disease compartments for the system are given by

$$\frac{dx}{dt} = \mathcal{F}(x,y) - \mathcal{V}(x,y)$$

and dynamics of infected compartments is given by

$$\frac{dx}{dt} = (F - V_\Gamma)x - f(x,y),$$

then $f(x,y)$ is obtained as follows;

$$\begin{aligned} f(x,y) &= (F - \mathcal{V}_\Gamma)x - \mathcal{F}(x,y) + \mathcal{V}(x,y) \\ &= \begin{pmatrix} \frac{BS\beta(f-1)}{B+K_B} - \frac{B\beta m_2\Lambda(f-1)}{K_B(m_1m_2-\omega\rho)} \\ \frac{B\beta f m_2\Lambda}{K_B(m_1m_2-\omega\rho)} - \frac{BS\beta f}{B+K_B} \\ 0 \\ 0 \end{pmatrix}, \end{aligned} \tag{3.3.12}$$

while

$$V_\Gamma^{-1}F = \begin{pmatrix} 0 & 0 & 0 & \frac{\beta m_2\Lambda(f-1)}{K_B m_3(\omega\rho - m_1m_2)} \\ 0 & 0 & 0 & \frac{\beta f m_2\Lambda}{K_B m_4(m_1m_2-\omega\rho)} \\ 0 & 0 & 0 & \frac{\beta m_2\Lambda\tau(f-1)}{K_B m_3 m_5(\omega\rho - m_1m_2)} \\ 0 & 0 & 0 & \frac{\beta f m_2\Lambda\varphi_a}{K_B m_4\mu_B(m_1m_2-\omega\rho)} - \frac{\beta m_2\Lambda\varphi_s(f-1)}{K_B m_3\mu_B(m_1m_2-\omega\rho)} \end{pmatrix}.$$

$F \geq 0$, $V_\Gamma^{-1} \geq 0$, $f(x,y) \geq 0$ and $f(x, \left(\frac{(\omega+\mu)\Lambda}{\mu(\rho+\omega+\mu)}, \frac{\rho\Lambda}{\mu(\rho+\omega+\mu)}, 0, 0\right)) = 0$ in Ω. It is also clear that $V_\Gamma^{-1}F$ is reducible. The Lyapunov function can be constructed based on Theorem 2.1 and 2.2 as stated by [92]. Eigenvectors of $V^{-1}F$ corresponding to the eigenvalue of $\mathcal{R}_C$ by $\{v_1, v_2, v_3, v_4\}$ can now be denoted.

Then

$$(v_1, v_1, v_1)\, V^{-1}F = \mathcal{R}_C\, (v_1, v_2, v_3, v_4)$$

or

$$(v_1, v_2, v_3, v_4)\, V^{-1} F = \begin{pmatrix} 0 & 0 & 0 & \frac{\beta f m_2 \Lambda \left(\frac{v_2}{m_4} + \frac{v_4 \varphi_a}{m_4 \mu_B}\right)}{K_B (m_1 m_2 - \omega\rho)} - \frac{\beta m_2 \Lambda (f-1) \left(\frac{v_1}{m_3} + \frac{\tau v_3}{m_3 m_5} + \frac{v_4 \varphi_s}{m_3 \mu_B}\right)}{K_B (m_1 m_2 - \omega\rho)} \end{pmatrix} \tag{3.3.13}$$

and

$$\mathcal{R}_C\,(v_1, v_2, v_3, v_4) = \frac{\beta m_2 \Lambda\,(m_4 \varphi_s (1-f) + f m_3 \varphi_a)}{K_B m_3 m_4 \mu_B (m_1 m_2 - \omega\rho)}\,(v_1, v_2, v_3, v_4)\,. \tag{3.3.14}$$

Using Equations (3.3.13) and (3.3.14) to derive a possible solution as $v_1 = 0$, $v_2 = 0, v_3 = 0$, and to allow workability, let $v_4 = \psi$, where ψ is a random parameter and is given by

$$\frac{\beta f m_2 \Lambda \psi \varphi_a}{K_B m_4 \mu_B (m_1 m_2 - \omega\rho)} + \frac{\beta m_2 \Lambda \left(\frac{\psi \varphi_s}{m_3 \mu_B}\right)(1-f)}{K_B (m_1 m_2 - \omega\rho)} = \frac{\beta m_2 \Lambda \psi\,(m_4 \varphi_s + f m_3 \varphi_a - f m_4 \varphi_s)}{K_B m_3 m_4 \mu_B (m_1 m_2 - \omega\rho)}. \tag{3.3.15}$$

Use Eq. (3.3.15) to obtain

$$\psi = \frac{m_4 \mu_B \psi (1-f)}{m_4 \varphi_s + f m_3 \varphi_a - f m_4 \varphi_s - m_3 m_5 \varphi_a - m_4 m_5 \varphi_s (1-f)}. \tag{3.3.16}$$

Therefore, $\Pi^T = (0, 0, 0, v_4)$. Thus, by Theorem 2.1 of [92], $\mathcal{Q} = \Pi^T V^{-1} x$ is the Lyapunov function of the model given by

$$\begin{aligned} \mathcal{Q} &= \Pi^T V_\Gamma^{-1} x \\ &= I_s \left(\frac{\tau}{m_3 m_5} + \frac{m_4 \tau \varphi_s (1-f)}{m_3 (m_4 \varphi_s + f m_3 \varphi_a - f m_4 \varphi_s - m_3 m_5 \varphi_a - m_4 m_5 \varphi_s (1-f))} \right) \\ &+ \frac{T}{m_5} + \frac{B m_4 \tau (1-f)}{m_4 \varphi_s (1-f)(1-m_5) + m_3 \varphi_a (f - m_5)} \\ &+ \frac{I_a}{m_4 \varphi_s} \left[\frac{\tau \varphi_a (1-f)}{(1-f)(1-m_5) + m_3 \varphi_a (f - m_5)} \right]. \end{aligned}$$

$\mathcal{Q}$ can be differentiated at DFE to get yields 0 since $I_{s_0} = 0 = I_{a_0} = T_0 = 0$ (see Equations (3.3.9c)-(3.3.9b))

$$\mathcal{Q}|'_{DFE} = (\mathcal{R}_C - 1)\,\Pi^T x - \Pi^T V_\Gamma^{-1} f(x,y) = 0. \tag{3.3.17}$$

This implies that $x = 0$ and $f(x,y) = 0$ or $y = (S,V,R)^\top = \left(\left(\frac{m_2\Lambda}{m_1m_2-\omega\rho}\right), \left(\frac{\Lambda\rho}{m_1m_2-\omega\rho}\right), 0\right)^\top$. Therefore, $\left(\left(\frac{m_2\Lambda}{m_1m_2-\omega\rho}\right), \left(\frac{\Lambda\rho}{m_1m_2-\omega\rho}\right) 0,0,0,0,0\right)$ is the only invariant set in Ω where $\mathcal{Q}' = 0$. Thus, by LaSalle's invariance principle [8], the DFE, $\left(\left(\frac{m_2\Lambda}{m_1m_2-\omega\rho}\right), \left(\frac{\Lambda\rho}{m_1m_2-\omega\rho}\right) 0,0,0,0,0\right)$ is globally asymptotically stable in Ω and $\mathcal{R}_C \leq 1$. □

LaSalle's invariance principle [11] is used to show that global stability of DFE is as follows; if $\mathcal{Q} = 0$, then

$$\left(\frac{\beta\tau(1-f)K_M}{K_Bm_3m_5(m_1m_2-\omega\rho)D_M}\right)\left(\frac{B(Bm_2\Lambda + K_Bm_2\Lambda - K_BSm_1m_2 + K_BS\omega\rho)}{B+K_B}\right) = (\mathcal{R}_C - 1)\,\Pi^T x, \tag{3.3.18}$$

where $K_M = m_4\varphi_s(1-f) + m_3\varphi_a\left((f-m_5)(1-m_5) - m_5^2)\right)$ and
$D_M = m_4\varphi_s(1-f)(1-m_5) + m_3\varphi_a(f-m_5)$. Since $(1-f) > 0; (1-m_5) > 0;\implies D_M > 0$ and $K_M \geq 0$.
Since $\mathcal{R}_C < 1$, then

$$\left(\frac{\beta\tau(1-f)K_M}{K_Bm_3m_5(m_1m_2-\omega\rho)D_M}\right)\left(\frac{B(Bm_2\Lambda + K_Bm_2\Lambda - K_BSm_1m_2 + K_BS\omega\rho)}{B+K_B}\right) \leq 0, \tag{3.3.19}$$

but $\left(\frac{\beta\tau(1-f)K_M}{K_Bm_3m_5(m_1m_2-\omega\rho)D_M}\right) > 0$ (substitution of parameter values), which implies that

$$\begin{aligned}
&\left(\frac{B(Bm_2\Lambda + K_Bm_2\Lambda - K_BSm_1m_2 + K_BS\omega\rho)}{B+K_B}\right) \leq 0\\
&\frac{B}{B+K_B}\left[\frac{Bm_2\Lambda + K_Bm_2\Lambda}{B+K_B} - \frac{K_BSm_1m_2 + K_BS\omega\rho}{B+K_B}\right] \leq 0\\
&\implies \Lambda m_2 \leq \frac{K_BS}{B+K_B}(m_1m_2 - \omega\rho) \leq S(m_1m_2 - \omega\rho).
\end{aligned} \tag{3.3.20}$$

Since $m_2, \mu, K_B, \omega, \rho > 0$, then its feasible that $B = 0$. Thus, $\{(\Lambda, 0, 0, 0, 0)\}$ is the only invariant

set in Ω which satisfies $\mathcal{Q}' = 0$ when $R_0 < 1$. Therefore, by LaSalle's invariance principle, the DFE is globally asymptotically in Ω when $\mathcal{R}_C < 1$ [63].

If $\mathcal{R}_C = 1$, then the RHS of Eq. (3.3.18) is zero, thus there is equality in Eq. (3.3.20). Therefore, $\{(\Lambda, 0, 0, 0, 0)\}$ is the only invariant set in Ω which satisfies $\mathcal{Q}' = 0$ when $\mathcal{R}_C = 1$. Thus, by LaSalle's invariance principle, the DFE is globally asymptotically in Ω when $\mathcal{R}_C = 1$ [63].

It can be shown that when $\mathcal{R}_C > 1$ and $\mathcal{Q}' > 0$, then Ω is in the neighborhood of X_0 where X_0 is the DFE, making X_0 unstable. For $\mathcal{R}_C > 1$, the first term of Eq. (3.3.17) becomes positive and second term zero when $S = V = N$ and $B = 0$, which proves that $\mathcal{Q}' > 0$. Therefore, by continuity, $\mathcal{Q}'$ remains positive in a small neighbourhood of X_0. This indicates that the system is globally asymptotically stable at X_0, which rules out the existence of backward bifurcation when $\mathcal{R}_C \geq 1$. Freedman *et al.* [34] argument of uniform persistence result based on the proof of proposition 3.3 of [59] whenever $\mathcal{R}_C > 1$ indicates instability of X_0 implying that the system is uniformly persistent. A uniform persistence and positive invariance of the compact set Ω implies the existence of at least one positive equilibrium.

3.3.3 Endemic Equilibrium

Let $S^*, V^*, I_s^*, I_a^*, T^*, R^*$ and B^* be endemic equilibrium of the system defined in Equations (3.1.2)-(3.1.8). Eq. (3.1.2) and Eq. (3.1.3) are used to obtain

$$S^* = \frac{m_2 \rho \Lambda}{m_1 m_2 - \omega \rho} \tag{3.3.21}$$

and

$$V^* = \frac{\rho \Lambda}{m_1 m_2 - \omega \rho}. \tag{3.3.22}$$

Eq. (3.3.11) is used to define $\left(m_1 m_2 - \omega \rho\right)$ as

$$(m_1 m_2 - \omega \rho) = \frac{\beta m_2 \Lambda \left(m_4 \varphi_s (1 - f) + f m_3 \varphi_a\right)}{\mathcal{R}_C K_B m_3 m_4 \mu_B}. \tag{3.3.23}$$

Eq. (3.3.23) is used to re-write Eq. (3.3.21) and Eq. (3.3.22) as

$$S^* = \frac{\mathcal{R}_C K_B m_3 m_4 \mu_B}{\beta(m_4\varphi_s(1-f) + f m_3 \varphi_a)}. \tag{3.3.24}$$

$$V^* = \frac{\rho \mathcal{R}_C K_B m_3 m_4 \mu_B}{\beta m_2(m_4\varphi_s(1-f) + f m_3 \varphi_a)}. \tag{3.3.25}$$

Eq. (3.3.24) and Eq. (3.3.25) are used to obtain I_s^*, I_a^*, T^*, R^* and B^* as follows;

$$I_s^* = \frac{K_B \mathcal{R}_C m_4 \mu_B (B^*\beta m_2 + K_B \rho\sigma\xi - B^*\beta f m_2 + B^*\rho\sigma\xi)}{(\beta m_2(B^* + K_B)(m_4\varphi_s + f m_3\varphi_a - f m_4\varphi_s)}, \tag{3.3.26}$$

$$I_a^* = \frac{K_B \mathcal{R}_C m_3 m_4 \mu_B (\rho\sigma(\xi - 1) - B^* f)}{(m_4\varphi_s(f-1) - f m_3\varphi_a)(B^* + K_B)\beta m_2}, \tag{3.3.27}$$

$$T^* = \frac{K_B \mathcal{R}_C m_4 \mu_B \tau (B^*\beta m_2 + K_B \rho\sigma\xi - B^*\beta f m_2 + B^*\rho\sigma\xi)}{\beta m_2 m_5(B^* + K_B)(m_4\varphi_s + f m_3\varphi_a - f m_4\varphi_s)}, \tag{3.3.28}$$

$$R^* = \frac{\begin{array}{l} K_B \mathcal{R}_C m_4 \mu_B (B^*\beta m_2 m_5 \theta_s + B^* f m_3 m_5 \theta_a + B^*\beta m_2 \tau\theta_t + m_3 m_5 \rho\sigma\theta_a \\ - m_3 m_5 \rho\sigma\theta_a\xi - B^*\beta f m_2 m_5 \theta_s - B^*\beta f m_2 \tau\theta_t \begin{array}{l} + B^* m_5 \rho\sigma\theta_s\xi + B^*\rho\sigma\tau\theta_t\xi \\ + K_B m_5 \rho\sigma\theta_s\xi + K_B\rho\sigma\tau\theta_t\xi) \end{array} \end{array}}{\beta m_2 m_5 \mu(B^* + K_B)(m_4\varphi_s + f m_3\varphi_a - f m_4\varphi_s)}, \tag{3.3.29}$$

and

$$B^* = \frac{(K_B \mathcal{R}_C m_4 \mu_B (m_3\rho\sigma\varphi_a + \beta m_2\varphi_s + f m_3\varphi_a - \beta f m_2\varphi_s + \rho\sigma\varphi_s\xi + K_B\rho\sigma\varphi_s\xi - m_3\rho\sigma\varphi_a\xi))}{(\beta m_2 \mu K_B)(m_4\varphi_s + f m_3\varphi_a - f m_4\varphi_s))}. \tag{3.3.30}$$

Global Stability of endemic equilibrium

Lemma 3.3.4. *When $\mathcal{R}_C > 1$, there exists a unique endemic equilibrium X^* given by $B^* = \frac{-b \pm \sqrt{b^2 - 4ac}}{2a}$, where $a = 2\left(m_2\pi_G\pi_r\pi_n^2 + m_2 m_4 \pi_D\right)$, $b = 2m_3\mu_B\pi_r\left(\mathcal{R}_C - 1\right)(\beta m_2 + m_1 m_2 - \omega\rho)$ and $c = -K_B\left(\mathcal{R}_C - 1\right)m_4\mu_B\pi_L\pi_n\pi_r\left(m_1 m_2 - \omega\rho\right)$. When $\mathcal{R}_C \leq 1$, there is no endemic equilibrium.*

Proof. Eq. (3.1.4) and Eq. (3.1.5) are used to obtain

$$0 = \frac{\varphi_a\left(\frac{B^* S^* \beta f}{B^* + K_B} - \frac{S^*\rho\sigma(\xi - 1)}{m_2}\right)}{m_4} - B^*\mu_B - \frac{\varphi_s\left(\frac{B^* S^*\beta(f-1)}{B^* + K_B} - \frac{S^*\rho\sigma\xi}{m_2}\right)}{m_3}. \tag{3.3.31}$$

Eq. (3.3.31) and Eq. (3.3.11) are used to get

$$S^* = \frac{B^*\mu_B}{\frac{\varphi_s(\pi_Q - R_0\pi_D)}{\pi_r(\pi_L - R_0\pi_n)} - \frac{\varphi_a\left(\frac{\pi_B}{m_2} + \frac{R_0\pi_G}{\pi_L - R_0\pi_n}\right)}{m_4}} \tag{3.3.32}$$

where

$\pi_m = m_1m_2 - \omega\rho$,$\pi_c = m_4\varphi_s(f-1) - fm_3\varphi_a$ $\pi_n = m_3m_4\mu_B\pi_m$, $\pi_L = \beta m_2\mu\pi_c$, $\pi_A = \rho\sigma\xi$, $\pi_H = m_2\pi_n$, $\pi_B = \rho\sigma(\xi - 1)$, $\pi_G = \beta f\pi_n$, $\pi_Z = \beta\pi_H$, $\pi_Q = \pi_L\pi_A$, $\pi_D = (\pi_Z + f - \pi_n\pi_A)$, $\pi_r = m_2m_3$.

Simplify Eq. (3.3.32) based on B^* to obtain

$$0 = aB^{*2} + bB^* + c, \tag{3.3.33}$$

where

$$a = 2(m_2\pi_G\pi_r\pi_n^2 - \pi_B\pi_r\pi_n + m_2m_4\pi_D) \tag{3.3.34a}$$

$$b = 2m_4\mu_B\pi_r(R_0 - 1)(\beta m_2 + m_1m_2 - \omega\rho) \tag{3.3.34b}$$

$$c = -K_B(R_0 - 1)m_4\mu_B\pi_L\pi_n\pi_r(m_1m_2 + \omega\rho). \tag{3.3.34c}$$

Eq. (3.3.33) suggests that there are two endemic equilibria as

$$B_1^* = \frac{-b+\sqrt{b^2-4ac}}{2a} \quad B_2^* = \frac{-b-\sqrt{b^2-4ac}}{2a}. \tag{3.3.35}$$

Eq. (3.3.35) indicates that the following cases are feasible;

1. When $\mathcal{R}_C > 1$, then

   $a > 0, c < 0$ and $b > 0$ if

$$\begin{aligned} &\Big(2m_4\mu_B\pi_r(\mathcal{R}_C - 1)(\beta m_2 + m_1m_2 - \omega\rho)\Big)^2 \\ &> 4\Big(2(m_2\pi_G\pi_r\pi_n^2 - \pi_B\pi_r\pi_n + m_2m_4\pi_D)\Big)\Big(-K_B(R_0 - 1)m_4\mu_B\pi_L\pi_n\pi_r(m_1m_2 + \omega\rho)\Big), \\ \implies\ & b^2 - 4ac > b^2. \end{aligned}$$

Suppose

$$\begin{aligned}
&\Big(2m_4\mu_B\pi_r(\mathcal{R}_C-1)(\beta m_2+m_1m_2-\omega\rho)\Big)^2\\
&<4\Big(2(m_2\pi_G\pi_r\pi_n^2-\pi_B\pi_r\pi_n+m_2m_4\pi_D)\Big)\Big(-K_B(R_0-1)m_4\mu_B\pi_L\pi_n\pi_r(m_1m_2+\omega\rho)\Big),\\
\implies\quad & b<0 \text{ and } b^2-4ac>b^2.
\end{aligned}$$

If

$$\begin{aligned}
&\Big(2m_4\mu_B\pi_r(\mathcal{R}_C-1)(\beta m_2+m_1m_2-\omega\rho)\Big)^2\\
&=4\Big(2(m_2\pi_G\pi_r\pi_n^2-\pi_B\pi_r\pi_n+m_2m_4\pi_D)\Big)\Big(-K_B(R_0-1)m_4\mu_B\pi_L\pi_n\pi_r(m_1m_2+\omega\rho)\Big),\\
\implies\quad & b=0 \text{ and } b^2-4ac=-4ac<0.
\end{aligned}$$

2. When $\mathcal{R}_C=1$:

   $a>0$, $c=0$ and $b>0$, thus $b^2-4ac=b^2$. There are no real roots.

3. When $\mathcal{R}_C<1$:

   $a>0$, $c>0$, and $b>0$, hence $b^2-4ac<0$. There are no real roots.

Table 3.2 summarizes the analytical solution of Eq. (3.3.33) based on $\mathcal{R}_C$.

Table 3.2: Analytical solution of Eq. (3.3.33).

$\mathcal{R}_\mathbf{C}$	**c**	**4ac**	**b**	$\mathbf{b^2-4ac}$	$\mathbf{-b+\sqrt{b^2-4ac}}$	$\mathbf{-b-\sqrt{b^2-4ac}}$	Comment
>1	<0	<0	$=0$	$-4ac>0$	>0	<0	1 EE
			<0	$>b^2$	>0	<0	1 EE
			>0	$>b^2$	>0	<0	1 EE
$=1$	$=0$	$=0$	>0	$=b^2$	$=0$	<0	no EE
<1	>0	$\in(0,b^2)$	>0	$\in(0,b^2)$	<0	<0	1 EE
		$\in(b^2,\infty)$	>0	<0	complex	complex	no EE

Table 3.2 shows that when $\mathcal{R}_C<1$, there is no endemic equilibrium, but if $\mathcal{R}_C>1$, a unique endemic equilibrium is obtained when

$$B^*=B_1^*=\frac{-b+\sqrt{b^2-4ac}}{2a}.$$

□

Theorem 3.4. *If $\mathcal{R}_C > 1$, the unique equilibrium is globally asymptotically stable in Ω.*

Proof. Proof of Volterra-Lyapunov is based on stable matrices according to [60]. The Lyapunov function is defined as follows;

$$L = \phi_1(S-S^*)^2+\phi_2(V-V^*)^2+\phi_3(I_s-I_s^*)^2+\phi_4(I_a-I_a^*)^2+\phi_5(T-T^*)^2+\phi_6(R-R^*)^2+\phi_7(B-B^*)^2 \tag{3.3.36}$$

where $\phi_i : \forall i = 1, \ldots, 7$ are positive constants. Differentiate L along the trajectories of the system to obtain

$$\begin{aligned} L \quad &= 2\phi_1(S-S^*)\left(\Lambda + \omega V - (m_1 + (\tfrac{\beta B}{K_B+B}))S\right) \\ &+2\phi_2(V-V^*)\left(\rho S - m_2 V\right) \\ &+2\phi_3(I_s-I_s^*)\left(\sigma\xi V + (1-f)(\tfrac{\beta B}{K_B+B})S - m_3 I_s\right) \\ &+2\phi_4(I_a-I_a^*)\left((1-\xi)\sigma V + f(\tfrac{\beta B}{K_B+B})S - m_4 I_a\right) \\ &+2\phi_5(T-T^*)\left(\tau I_s - m_5 T\right) \\ &+2\phi_6(R-R^*)\left(\theta_t T + \theta_a I_a + \theta_s I_s - \mu R\right) \\ &+2\phi_7(B-B^*)\left(\varphi_a I_a + \varphi_s I_s - \mu_B B\right). \end{aligned} \tag{3.3.37}$$

Use Eq. (3.3.37) to compute Eq. (3.3.38) as follows;

$$\begin{aligned}
L^{'} &= -2\phi_1(S-S^*)^2\left(m_1+(\tfrac{\beta B}{K_B+B})\right)+2\phi_1(S-S^*)(V-V^*)\omega \\
&-2\phi_1(S-S^*)(B-B^*)\left(\tfrac{\beta}{(B+K_B)}-\tfrac{B\beta}{(B+K_B)^2}\right)S \\
&+2\phi_2(V-V^*)(S-S^*)\rho-2\phi_2(V-V^*)^2m_2 \\
&+2\phi_3(I_s-I_s^*)(S-S^*)(1-f)\tfrac{\beta B}{K_B+B}+2\phi_3(I_s-I_s^*)(V-V^*)\sigma\xi-2\phi_3(I_s-I_s^*)^2m_3 \\
&+2\phi_3(I_s-I_s^*)(B-B^*)(1-f)S\left(\tfrac{\beta}{(B+K_B)}-\tfrac{B\beta}{(B+K_B)^2}\right) \\
&+2\phi_4(I_a-I_a^*)(S-S^*)f\tfrac{\beta B}{K_B+B}+2\phi_4(I_a-I_a^*)(V-V^*)(1-\xi)\sigma-2\phi_4(I_a-I_a^*)^2m_4 \\
&+2\phi_4(I_a-I_a^*)(B-B^*)fS\left(\tfrac{\beta}{(B+K_B)}-\tfrac{B\beta}{(B+K_B)^2}\right) \\
&+2\phi_5(T-T^*)(I_s-I_s^*)\tau-2\phi_5(T-T^*)^2m_5+2\phi_6(R-R^*)(I_s-I_s^*)\theta_s \\
&+2\phi_6(R-R^*)(I_a-I_a^*)\theta_a+2\phi_6(R-R^*)(T-T^*)^2\theta_t-2\phi_6(R-R^*)^2\mu \\
&+2\phi_7(B-B^*)(I_s-I_s^*)\varphi_s+2\phi_7(B-B^*)(I_a-I_a^*)\varphi_a-2\phi_7(B-B^*)^2\mu_B \\
&= \Psi(\Phi\Gamma+\Gamma^T\Phi^T)\Psi^T,
\end{aligned} \tag{3.3.38}$$

where $\Psi=(S-S^*,V-V^*,I_s-I_s^*,I_a-I_a^*,T-T^*,R-R^*,B-B^*$, $\Phi=diag\,(\phi_1,\phi_2,\phi_3,\phi_4,\phi_5,\phi_6,\phi_7)$ and

$$\Gamma=\begin{pmatrix}
-\left(m_1+(\tfrac{\beta B}{K_B+B})\right) & \omega & 0 & 0 & 0 & 0 & \left(\tfrac{\beta}{(B+K_B)}-\tfrac{B\beta}{(B+K_B)^2}\right)S \\
\rho & -m_2 & 0 & 0 & 0 & 0 & 0 \\
(1-f)\tfrac{\beta B}{K_B+B} & \sigma\xi & -m_3 & 0 & 0 & 0 & (1-f)S\left(\tfrac{\beta}{(B+K_B)}-\tfrac{B\beta}{(B+K_B)^2}\right) \\
f\tfrac{\beta B}{K_B+B} & (1-\xi)\sigma & 0 & -m_4 & 0 & 0 & fS\left(\tfrac{\beta}{(B+K_B)}-\tfrac{B\beta}{(B+K_B)^2}\right) \\
0 & 0 & \tau & 0 & -m_5 & 0 & 0 \\
0 & 0 & \theta_s & \theta_a & \theta_t & -\mu & 0 \\
0 & 0 & \varphi_s & \varphi_a & 0 & 0 & -\mu_B
\end{pmatrix}. \tag{3.3.39}$$

$$det(\Gamma)=\frac{-m_5\mu\left(\Sigma_1+\Sigma_2+\Sigma_3+\Sigma_4-\Sigma_5+\Sigma_6+\Sigma_7+\Sigma_8+\Sigma_9-\Sigma_{10}+\Sigma_{11}+\Sigma_{12}\right)}{(B+K_B)^3} \tag{3.3.40}$$

where

$$\Sigma_1 = B^3\left(\eta_1+\eta_2-\eta_3\right), \qquad \Sigma_2 = K_B^3\eta_2 - K_B^3\eta_3 - 2BK_BS\beta^2 m_2m_4\varphi_s,$$
$$\Sigma_3 = BK_B^2\eta_1 + 2B^2K_B\eta_1 + 3BK_B^2\eta_2, \qquad \Sigma_4 = 3B^2K_B\eta_2 - 3BK_B^2\eta_3 - 3B^2K_B\eta_3,$$
$$\Sigma_5 = K_B^2S\eta_4 + K_B^2S\eta_{12} - K_B^2S\eta_{11}, \qquad \Sigma_6 = K_B^2S\eta_9 - K_B^2S\eta_{10} - BK_BS\eta_4,$$
$$\Sigma_7 = BK_BS\eta_{12} - BK_BS\eta_{11} - 2BK_BS\beta^2 f m_2m_3\varphi_a, \qquad \Sigma_9 = K_B^2S\eta_5 - K_B^2S\eta_8$$
$$\Sigma_8 = 2BK_BS\beta^2 f m_2m_4\varphi_s - K_B^2S\eta_6 + K_B^2S\eta_7, \qquad \Sigma_{10} = BK_BS\eta_6 + BK_BS\eta_7,$$
$$\Sigma_{11} = BK_BS\eta_5 - BK_BS\eta_8, \qquad \Sigma_{12} = BK_BS\eta_9 - BK_BS\eta_{10}$$

and

$$\eta_1 = \beta m_2m_3m_4\mu_B, \quad \eta_2 = m_1m_2m_3m_4\mu_B, \quad \eta_3 = m_3m_4\mu_B\omega\rho, \quad \eta_4 = \beta m_1m_2m_4\varphi_s,$$
$$\eta_5 = \beta f m_3\omega\rho\varphi_a, \quad \eta_6 = \beta f m_1m_2m_3\varphi_a, \quad \eta_7 = \beta f m_1m_2m_4\varphi_s, \quad \eta_8 = \beta f m_4\omega\rho\varphi_s,$$
$$\eta_9 = \beta m_3\rho\sigma\varphi_a\xi, \quad \eta_{10} = \beta m_4\rho\sigma\varphi_s\xi, \quad \eta_{11} = \beta m_3\rho\sigma\varphi_a, \quad \eta_{12} = \beta m_4\omega\rho\varphi_s.$$

From Eq. (3.1.3), Eq. (3.1.4), Eq. (3.1.5) and Eq. (3.1.8) and considering the equilibrium $(S^*.V^*, I_s^*, I_a^*, T^*, R^*, B^*)$, it is noted that

$$\rho S^* - m_2V^* = 0 \implies V^* = \frac{\rho S^*}{m_2} \tag{3.3.41}$$
$$\sigma\xi V^* + (1-f)\left(\frac{\beta B}{K_B+B}\right)S^* - m_3I_s^* = 0 \tag{3.3.42}$$
$$(1-\xi)\sigma V^* + f\left(\frac{\beta B}{K_B+B}\right)S^* - m_4I_a^* = 0 \tag{3.3.43}$$
$$\varphi_aI_a^* + \varphi_sI_s^* - \mu_BB^* = 0. \tag{3.3.44}$$

Substitution of Eq. (3.3.41) into Eq. (3.3.42) and Eq. (3.3.43) gives

$$\begin{aligned} I_s^* &= \tfrac{\sigma\xi\rho S^*}{m_2m_3} + \tfrac{(1-f)\beta B^*S^*}{(K_B+B^*)m_3} \\ I_a^* &= \tfrac{\sigma(1-\xi)\rho S^*}{m_2m_4} + \tfrac{f\beta B^*S^*}{(K_B+B^*)m_4}. \end{aligned} \tag{3.3.45}$$

Suppose $B \geq 0$ and $B = 0$, then we have

$$\begin{aligned} I_s^* &= \frac{\sigma\xi\rho S^*}{m_2 m_3} \\ I_a^* &= \frac{\sigma(1-\xi)\rho S^*}{m_2 m_4}. \end{aligned} \tag{3.3.46}$$

Substitution of Eq. (3.3.46) into Eq. (3.3.44) and considering $B = 0$ gives

$$\varphi_s \frac{\sigma\xi\rho S^*}{m_2 m_3} + \varphi_a \frac{\sigma(1-\xi)\rho S^*}{m_2 m_4} = 0. \tag{3.3.47}$$

Eq. (3.3.47) is not feasible, since $\frac{\sigma\rho S^*}{m_2 m_4}\Big[\xi\varphi_s + (1-\xi)\varphi_a\Big] \neq 0$, hence $B > 0 \implies det(\Gamma) > 0$. Therefore, $\Phi(-\Gamma) + [\Phi(-\Gamma)]^T > 0$, which implies that matrix Γ is Volterra-Lyapunov stable and Φ is a constant matrix. Thus, when $\mathcal{R}_C > 1$, the endemic equilibrium of the system is globally asymptotically stable in Ω. □

Chapter 4

Numerical Simulation

4.1 Sensitivity analysis of parameters

We use parameter values in Table 4.1 to perform a sensitivity analysis of parameters in control reproduction number $\mathcal{R}_C$ (Eq. (3.3.11)). Strength of the model is the incorporation of an improved environment to reduce the spread of cholera in Kenya.

4.1.1 Estimation of parameter values

Referring to the study area, Kenya, whose data is used in this research, the constant population is considered to be $N = 1000$. Assumed life expectancy is 67 years for the Kenyan population. The baseline parameter values are considered based on different sources outlined in Table 4.1. The ingestion rate of cholera pathogen β due to contact with contaminated sources is assumed from Hailemariam *et al.* [38] as 0.95. Cholera has no incubation period, hence the exposure compartment was not considered. A simulation of the model dynamics presented in Figure 4.1 and Figure 4.2 for assumed 52 weeks (1 year) shows a resemblance with other state-of-the-art methods.

Table 4.1: Parameter Values Baseline and Sources whose descriptions are in Table 3.1.

Parameter	**Values baseline**	**Values range**	**Source**
Λ	31.309	$51.27 - 31.31$ per 1000 people	[56]
f	0.79	-	Calculated
K_B	10^6	$10^5 - 10^6$	[98]
σ	28%	$8 \rightarrow 75\%$)	[86]
θ_a	0.1	$0 - 1$	[91]
ω	33%	$0 - 60\%$	[85]
ρ	1 per 14 days	$1 - 2$ per 14 days	[28]
ξ	0.15	$0.1 - 0.4$	[77]
θ_s	0.1	$0 - 0.3$	[91]
τ	0.20619	$0 - 0.4$	[21, 89]
θ_t	0.725444	-	Calculated
μ_B	0.033 per days	- days	[79]
φ_a	10^3	$1 - 10^5$ cells per day	[76]
φ_s	10^8	$10^7 - 10^9$	[76]
φ_t	10^5	$10^7 - 10^9$	[76]
β	1	$1 - 10^9$	[38]
μ	$9.1 \times 10^{-}(6)$	$5.732 - 20.21$ per 1000 people	[56]

4.1.2 Elasticity indices

Elasticity index ζ of parameter ν_i is given by $\frac{\nu_i \partial \mathcal{R}_C}{\mathcal{R}_C \partial \nu_i}$. ζ is a measure of the relative change in $\mathcal{R}_C$ to relative change in ν_i. ν_i with the largest absolute magnitude having higher influence on $\mathcal{R}_C$ and affects transmission dynamics of cholera as indicated in Theorem 3.2 and Theorem 3.4. Table 4.2 shows elasticity indices of parameters computed based on the baseline given in Table 4.1 with assumed N=1000. The table shows the indices arranged in descending order based on magnitude. The table shows that ingestion rate of *Vibrio cholerae* β has the largest magnitude, thus affecting cholera dynamics, followed by the rate of natural loss of *Vibrio cholerae*.

4.2 Numerical simulations for model analysis

Numerical simulations are presented to illustrate analysis of the model. Equations (3.1.2)-3.1.8 are presented in two cases based on baseline values in Table 4.1 when $\mathcal{R}_C > 1$ (Figure 4.1) and when $\mathcal{R}_C < 1$ (Figure 4.2).

Table 4.2: Elasticity indices of parameters in $\mathcal{R}_C$

Parameter	Elasticity Index
β	1.0000
μ_B	0.8931
ρ	-0.8612
τ	-0.6611
θ_a	0.0011
φ_s	0.00085
φ_a	0.00061

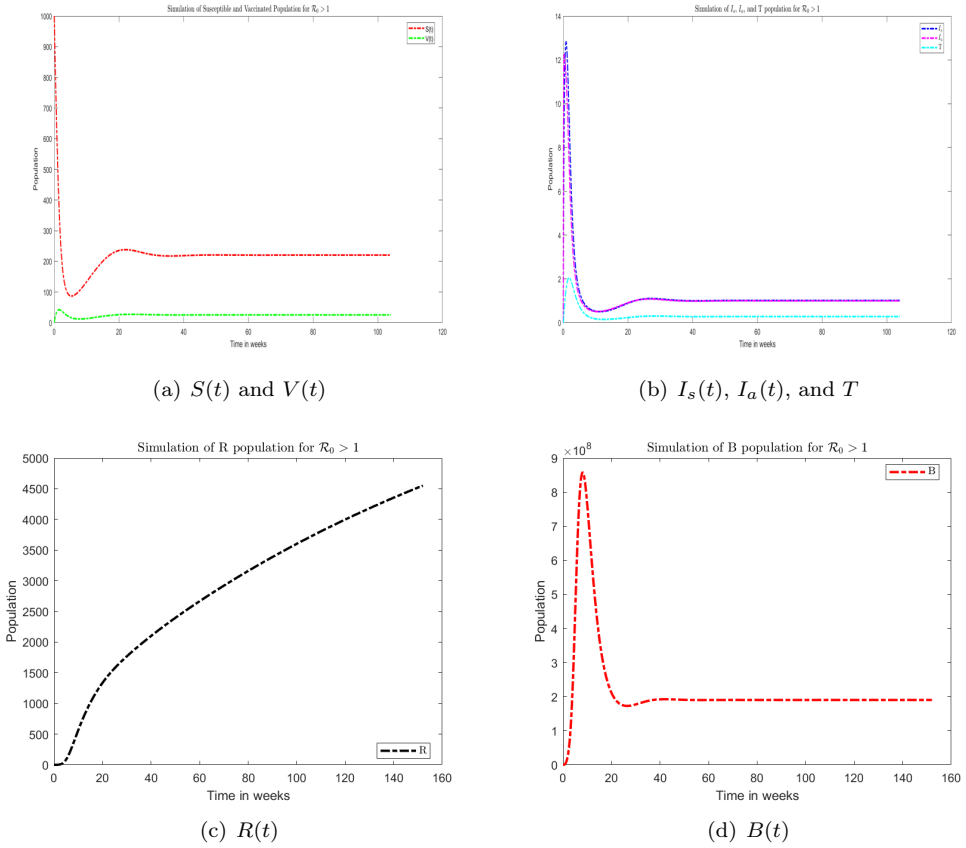

(a) $S(t)$ and $V(t)$

(b) $I_s(t)$, $I_a(t)$, and T

(c) $R(t)$

(d) $B(t)$

Figure 4.1: Simulation of the population of individuals in each compartment $S(t)$, $V(t)$, $I_s(t)$, $I_a(t)$, $T(t)$, $R(t)$ and $B(t)$ based on parameter values in Table 4.1 with initial conditions: $S_0 = 1000$, $V_0 = I_{s_0} = I_{a_0} = T_0 = R_0 = 0$, $B_0 = 10^5$ and $N = 1000$. $\beta = 0.95$ resulting in approximated equilibrium values of $S^* = 289$, $V^* = 26$, $I_s^* = I_a^* \simeq 2$, $T^* = 1$, $B^* = 1.9 \times 10^8$. and $\mathcal{R}_C = 1.5665$.

Figure 4.1 considers higher ingestion rate $\beta = 0.95$ and yields $\mathcal{R}_C = 1.5665$ with trajectories reaching unique endemic equilibrium values of $S^* = 289$, $V^* = 26$, $I_s^* \simeq I_a^* = 2$, $T^* = 2$ and

$B^* = 1.9 \times 10^8$.

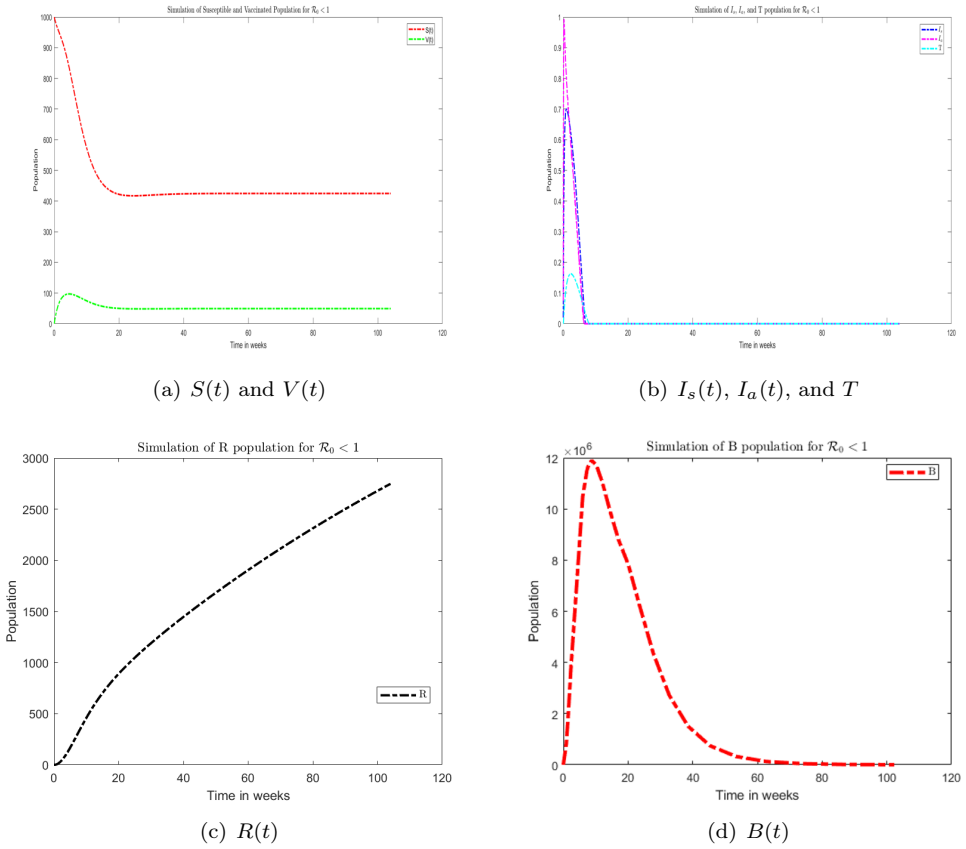

(a) $S(t)$ and $V(t)$ (b) $I_s(t)$, $I_a(t)$, and T

(c) $R(t)$ (d) $B(t)$

Figure 4.2: Simulation of the population of individuals in each compartment $S(t)$, $V(t)$, $I_s(t)$, $I_a(t)$, $T(t)$, $R(t)$ and $B(t)$ based on parameter values in Table 4.1 with initial conditions: $S_0 = 1000$, $V_0 = I_{s_0} = I_{a_0} = T_0 = R_0 = 0$, $B_0 = 10^5$ and $N = 1000$. $\beta = 0.19$ resulting in approximated equilibrium values of $S^* \simeq 425$, $V^* = 49$, $I_s^* = I_a^* = T^* = B^* = 0$ and $\mathcal{R}_C = 0.3133$.

Figure 4.2 considers the assumed effect of reduced sanitation (a case of global stability for DFE) $\beta = 0.19$ and yields $\mathcal{R}_C = 0.3133 < 1$ with trajectories reaching unique endemic equilibrium values of $S^* \simeq 425$, $V^* = 49$ and $I_s^* = I_a^* = T^* = B^* = 0$. In both cases (Figure 4.1 and Figure 4.2), trajectories approach equilibrium, an indication of stability of DFE in most cases of state variables.

Chapter 5

Optimal control to cholera model

Optimal control of cholera epidemic modelling is a critical approach to mitigating and managing the spread of the disease. Cholera is characterized by severe diarrhoea and can lead to dehydration and, in extreme cases, death. Developing strategies to control cholera is essential for public health officials, epidemiologists and policymakers. Unlike many other diseases, control of a cholera epidemic relies on reducing the ingestion rate of *Vibrio cholerae* pathogen by the population. Reduction in ingestion rate can be achieved by improving sanitation and hygiene. Thus, optimal control is achieved by extending the model Equations (3.1.2)-(3.1.8) to include the effect of improved sanitation to reduce ingestion rate of *V. cholerae* pathogen.

5.1 Introduction of controls

Table 4.2 shows that ingestion rate of *Vibrio cholerae* by humans is due to contact with contaminated sources. β has the highest elasticity index followed by the rate of natural loss of *Vibrio cholerae*. Therefore, the control considers sanitation and hygiene factors since they will reduce ingestion rate of *Vibrio cholerae* pathogen and its population within the environment. Thus a reduction of β and increase of μ_B are the main infection reduction strategies. While WHO specifies that the major treatment of cholera is oral or intravenous hydration, this study focuses on improvement in hygiene and sanitation.

Hygiene Let $h \in [0,1]$ (where h is an arbitrary letter used to indicate the control due to hygiene) be time-dependent and Lebesgue measurable control representing an improvement in hygienic efforts that reduce the chance of *V. cholerae* pathogen spread. Improved hygiene includes washing hands with soap after using the toilet and not sharing plates during meals. The set of admissible hygiene control is:

$$H = h(t) : [0,T] \longrightarrow [0,1] \text{ and is Lebesgue measurable.}$$

Sanitation Let $\vartheta \in [0,1]$ (where ϑ is an arbitrary letter used to indicate the control due to sanitation) be time-dependent and Lebesgue measurable control that represents sanitation efforts that reduce the chance of virus ingestion. Improved sanitation efforts include improved hygiene and provision of safe water for domestic and industrial use.
The admissible set of sanitation control is:

$$Q = q(t) : [0,T] \longrightarrow [0,1] \text{ and is Lebesgue measurable.}$$

For simplicity, control $u = (\vartheta, h)$ denotes control and the set of admissible controls $U = Q \times H$.

5.2 The extended mathematical model

Improvement in hygiene reduces ingestion and spread of the pathogen and is given by $h\beta$. Thus, the portion practising improved hygiene is $h\frac{\beta BS}{K_B+B}$. Improved sanitation reduces the portion of the pathogen ingested by those susceptible leading to reduced infection. Thus, qB represents pathogen loss due to sanitation.

$$\frac{dS}{dt} = \Lambda + \omega V - \left(\rho + \mu + (1-h)\frac{\beta B}{K_B + B}\right) S \tag{5.2.1}$$

$$\frac{dV}{dt} = \rho S - (\omega + \mu + \sigma)V \tag{5.2.2}$$

$$\frac{dI_s}{dt} = \sigma\xi V + (1-f)(1-h)\frac{\beta B}{K_B + B}S - (\theta_s + \tau + \mu)I_s \tag{5.2.3}$$

$$\frac{dI_a}{dt} = (1-\xi)\sigma V + f(1-h)\frac{\beta B}{K_B + B}S - (\theta_a + \mu)I_a \tag{5.2.4}$$

$$\frac{dT}{dt} = \tau I_s - (\mu + \theta_t)T \tag{5.2.5}$$

$$\frac{dR}{dt} = \theta_t T + \theta_a I_a + \theta_s I_s - \mu R \tag{5.2.6}$$

$$\frac{dB}{dt} = \varphi_a I_a + \varphi_s I_s - (\mu_B + q)B \tag{5.2.7}$$

with initial conditions

$$S(0) = S_0 V(0) = V_0, I_s(0) = I_{s0}, I_a(0) = I_{a0}, T(0) = T_0, R(0) = R_0, B(0) = B_0. \tag{5.2.8}$$

Intervention needs to minimize the number of new cases and also minimize the cost of implementing controls. The cost may include improving sanitation, such as repairs of leaking systems and provision of hand-wash facilities with soap at the toilets in case of informal settlements. Thus, the control $u = (q, h)$ is considered optimal if it minimizes the objective function:

$$J = \int_0^T \left(A_1\left[(1-h)\frac{\beta B}{K_B + B}S\right] + A_2 q^2 + A_3 h^3\right) dt \tag{5.2.9}$$

where A_1 is the unit cost of new infection per individual, $A_2 = A_3$ is the unit cost of implementing the controls per time unit. A_1, A_2 and A_3 are the balancing of coefficients that transforms the integrand into cost per time unit and $(1-h)\frac{\beta B}{K_B+B}S$ represents the cost of new cases. Thus, the optimal control problem is stated as follows:

$$\min_{u \in U} J(u) \tag{5.2.10}$$

subject to Equations (5.2.1) - (5.2.8).

5.3 Existence of optimal control

Theorem 5.1. *There exists an optimal control u^* and the corresponding solution $(S^*, V^*, I_s^*, I_a^*, T^*, R^*, B^*)$ to the initial value problem given by Equations* (5.2.1)-(5.2.7) *that minimizes the objective function given by Eq.* (5.2.9) *on U.*

Proof. The initial value problem reflected in Equations (5.2.1)-(5.2.7) can be written as

$$X^{'} = f(t, X, u),$$
$$\text{with } X(0) = X_0.$$

Results of Theorem 4.1 in [12] is used to establish existence of optimal control based on the following conditions;

1. There exist $\mathcal{C}_1$ and $\mathcal{C}_2$ such that

   a $|f(t, X, u)| \leq \mathcal{C}_1(1 + X)$ and

   b $|f(t, X_1, u)| - |f(t, X_2, u)| \leq \mathcal{C}_1|X_1 - X_2|$,

   $$\forall t \geq 0, X_1, X_2 \in \left\{ \left(S, V, I_s, I_a, R, T, B \in \mathbb{R}_+^7 \middle| S + V + I_s + I_a + T + R = N, B \leq \frac{(\varphi_a + \varphi_b)N}{\mu_B} \right) \right\}$$

   and $u \in U$, where $U = \left\{ u = (q, h) : 0 \leq q, h \leq 1 \right\}$.

2. The set of controls and corresponding state variables is non-empty.

3. The control set U is convex and closed, $f(t, X, u) = \alpha_1(t, X) + \beta_1(t, X)u$ and L is convex on U, where $L = A_1 \left[(1 - h)\frac{\beta B}{K_B + B} S \right] + A_2 q(t)^2 + A_3 h(t)^3$ which is the integrand in Eq. (5.2.9).

4. There exists $\mathcal{C}_3 > 0, \mathcal{C}_4 > 1$ and $\mathcal{C}_5 \geq 0$ such that

$$L(t, X, u) \geq \mathcal{C}_3|u|^{\mathcal{C}_4} - \mathcal{C}_5. \tag{5.3.1}$$

Since f is $\mathcal{C}^1$, conditions 1(a) and 1(b) are implied by suitable bounds on partial derivatives of f and on $f(t,0,0)$. Since f is continuous and bounded on a finite time interval, Theorem 9.2.1 of [62] guarantees the existence of at least one local solution. The set $U = \{(q,h) : q \in [0,1] \text{ and } h \in [0,1]$ is closed. By definition, the set $Q = \{q : q \in [0,1]$ is Lebesgue measurable$\}$ and convex if $q_1, q_2 \in Q$ and $\gamma_1 \in [0,1]$ implying that $\Big[1-\gamma_1)q_1 + \gamma_1 q_2 \in Q\Big]$

$(1-\gamma_1)q_1 + \gamma_1 q - 2 \geq 0$ since $\gamma_1, q_1, q_2 \in [0,1]$,

and

$(1-\gamma_1)q_1 + \gamma_1 q_2 \leq (1-\gamma_1) + \gamma_1$ since $q_1, q_2 \leq 1$.

Therefore, $(1-\gamma_1)q_1 + \gamma_1 q_2$ lying in Q implies that Q is convex. Similarly, Q is convex since according to [48] the Cartesian of convex sets is convex, thus $U = Q \times H$ is a convex set. The function f is linear in each control variable q and h, hence can be written as $f(t,X,u) = \alpha_1(t,X) + \beta_1(t,X)u$. L is convex on U since it is quadratic in u and the constants A_3 and A_5 are positive. Therefore,

$$\begin{aligned} L = \quad & A_1\Big[(1-h)\tfrac{\beta B}{K_B+B}S\Big] + A_2q^2 + A_3h^2 \\ \leq \quad & A_2q^2 + A_3h^2 + A_1\Big[(1-h)\tfrac{\beta B}{K_B+B}S\Big] \text{ since } q \geq 0, h \geq 0. \end{aligned} \tag{5.3.2}$$

It is taken into consideration that

$$\begin{aligned} A_1\Big[\tfrac{\beta B}{K_B+B}S\Big] \leq \quad & A_1\Big[(1-h)\tfrac{\beta B}{K_B+B}S\Big] \text{ since } q \leq 1 \textit{ and } h \leq 1 \\ \leq \quad & A_1\Big[(1-h)\tfrac{\beta B}{K_B+B}S\Big] \text{ since} \tfrac{\beta B}{K_B+B} \leq \tfrac{B}{K_B}. \\ & \leq A_1\Big[\tfrac{\beta(\varphi_a+\varphi_s)N^2}{K_B\mu_B}\Big] \text{ since } S \leq N \text{ and } B \leq \tfrac{(\varphi_a+\varphi_s)N}{\mu_B}. \end{aligned} \tag{5.3.3}$$

Both sides of inequality are non-negative, thus,

$$A_1\Big[(1-h)\frac{\beta B}{K_B+B}S\Big] \geq -A_1\Big[\frac{\beta B}{K_B+B}S\Big]. \tag{5.3.4}$$

Substitute Eq. (5.3.4) into Eq. (5.3.2) to have

$$\begin{aligned} L \quad & \leq A_2q(t)^2 + A_3h(t)^2 - A_1\Big[\tfrac{\beta(\varphi_a+\varphi_s)N^2}{K_B\mu_B}\Big] \\ & \geq \mathcal{C}_3|u|_4^{\mathcal{C}} - \mathcal{C}_5 \end{aligned} \tag{5.3.5}$$

where $\mathcal{C}_3 = \min A_2, A_3$, $calC_4 = 2$ and $\mathcal{C}_5 = A_1\left[\frac{\beta(\varphi_a+\varphi_s)N^2}{K_B\mu_B}\right]$.

□

5.4 Characterization of controls

Pontryagin's Maximum principle stated in Theorem 5.1 of [12] is used to find the best possible control for the system. Then define the Hamiltonian H as follows;

$$\begin{aligned} H(X,u,p) &= f(t,X,u) + L(t,X,u) \\ &= p_1 f_1 + p_2 f_2 + p_3 f_3 + p_4 f_4 + p_5 f_5 + p_6 f_6 + p_7 f_7 + L \\ &= p_1\left[\Lambda + \omega V - (m_1 + (1-h)\tfrac{\beta B}{K_B+B})S\right] \\ &+p_2\left[\rho S - m_2 V\right] \\ &+p_3\left[\sigma\xi V + (1-f)(1-h)\tfrac{\beta B}{K_B+B}S - m_3 I_s\right] \\ &+p_4\left[(1-\xi)\sigma V + f(1-h)\tfrac{\beta B}{K_B+B}S - m_4 I_a\right] \\ &+p_5\left[\tau I_s - m_5 T\right] \\ &+p_6\left[\theta_t T + \theta_a I_a + \theta_s I_s - \mu R\right] \\ &+p_7\left[\varphi_a I_a + \varphi_s I_s - (\mu_B + q)B\right] \\ &+A_1\left[(1-h)\tfrac{\beta B}{K_B+B}S\right] + A_2 q^2 + A_3 h^2 \end{aligned} \tag{5.4.1}$$

where $p = (p_1, p_2, p_3, p_4, p_5, p_6, p_7)$ and $p_1, p_2, p_3, p_4, p_5, p_6, p_7$ are adjoint variables for the state variable S, V, I_s, I_a, T, R and B.

Theorem 5.2. *Given an optimal solution (X^*, u^*) of the control problem Eq. (5.2.10), there exists $p_1, p_2, p_3, p_4, p_5, p_6$ and p_7, a solution set to the adjoint system*

$$
\begin{aligned}
\dot{p_1} &= -\tfrac{\partial H}{\partial S} = p_1 m_1 - (1-h)\tfrac{\beta B}{K_B+B}\Big[p_2\rho + p_3(1-f) + p_4 f + A_1\Big] \\
\dot{p_2} &= -\tfrac{\partial H}{\partial V} = -p_1\omega + p_2 m_2 - p_3\sigma\xi - p_4(1-\xi)\sigma \\
\dot{p_3} &= -\tfrac{\partial H}{\partial I_s} = p_3 m_3 - p_5\tau - p_6\theta_s - p_7\varphi_s \\
\dot{p_4} &= -\tfrac{\partial H}{\partial I_a} = p_4 m_4 - p_6\theta_a - p_7\varphi_a \\
\dot{p_5} &= -\tfrac{\partial H}{\partial T} = p_5 m_5 - p_6\theta_t \\
\dot{p_6} &= -\tfrac{\partial H}{\partial R} = p_6\mu \\
\dot{p_7} &= -\tfrac{\partial H}{\partial B} = -\left((1-h)\left[\tfrac{\beta}{(B+K_B)} - \tfrac{B\beta}{(B+K_B)^2}\right]S\right)\Big[p_1 + p_3(1-f) + p_4 f + A_1\Big] + p_7(\mu_B + q),
\end{aligned}
\tag{5.4.2}
$$

with transversality condition

$$
p_1(T) = 0,\ p_2(T) = 0,\ p_2(T) = 0,\ p_4(T) = 0,\ p_5(T) = 0,\ p_6(T) = 0,\ p_7(T) = 0,
$$

such that $u^* = \min_{u\in U} H(X, p, u)$, $t \in [0, T]$. Furthermore, controls can be characterized as
$q^* = \min\left(1, \max\left(0, \frac{p_7 B}{2A_2}\right)\right)$ and
$h^* = \min\left(1, \max\left(0, \frac{1}{2A_3}\left[\frac{\beta BS}{K_B+B}\left(p_3 + p_4 + A_1 - p_1\right)\right]\right)\right)$.

Proof. The optimal control is derived from the optimality condition $\left.\frac{\partial H}{\partial u}\right|_{u^*} = 0$.

$$
\begin{aligned}
\left.\tfrac{\partial H}{\partial q}\right|_{q^*} &= -p_7 B + 2A_2 q^* \\
\implies \qquad q^* &= \tfrac{p_7 B}{2A_2}
\end{aligned}
\tag{5.4.3}
$$

and

$$
\begin{aligned}
\left.\tfrac{\partial H}{\partial h}\right|_{q^*} &= \tfrac{\beta BS}{K_B+B}\left(p_3 + p_4 + A_1 - p_1\right) + 2A_3 h^* \\
\implies \quad h^* &= \tfrac{1}{2A_3}\left[\tfrac{\beta BS}{K_B+B}\left(p_3 + p_4 + A_1 - p_1\right)\right].
\end{aligned}
\tag{5.4.4}
$$

Consider the properties of the control space as

$$q^* = \begin{cases} 0, & \text{if } \frac{p_7 B}{2A_2} \geq 0, \\ \frac{p_7 B}{2A_2} & \text{if } 0 < \frac{p_7 B}{2A_2} < 1, \\ 1 & \text{if } \frac{p_7 B}{2A_2} \geq 1. \end{cases} \tag{5.4.5}$$

Thus, q^* can be characterized as

$$q^* = \min\left(1, \max\left(0, \frac{p_7 B}{2A_2}\right)\right).$$

Similarly, h^* can be characterized as

$$h^* = \min\left(1, \max\left(0, \frac{1}{2A_3}\left[\frac{\beta B S}{K_B + B}\left(p_3 + p_4 + A_1 - p_1\right)\right]\right)\right).$$

It is also noted from Eq. (5.4.3) and Eq. (5.4.4) respectively that
$\left.\frac{\partial^2 H}{\partial q^2}\right|_{q^*} = 2A_2 > 0$ and

$\left.\frac{\partial^2 H}{\partial h^2}\right|_{h^*} = 2A_3 > 0$. Since A_2 and A_3 are positive constants introduced in Eq. (5.2.9), this indicates that $u^* = (q^*, h^*)$ minimises the Hamiltonian function $H(X, p, u)$. □

5.5 Numerical simulation for optimal control

The optimal problem (Eq. (5.2.10)) was solved numerically based on parameter values in Table 4.1. Numerical solutions were compared with optimal control and without any intervention. The compartments are plotted side by side in the presence and absence of control measures $q \in [0, 1]$ and $h \in [0, 1]$ with $S_0 = 1000$, $V_0 = I_{s_0} = I_{a_0} = T_0 = R_0 = 0$, $B_0 = 0.7$ and $N = 1000$.

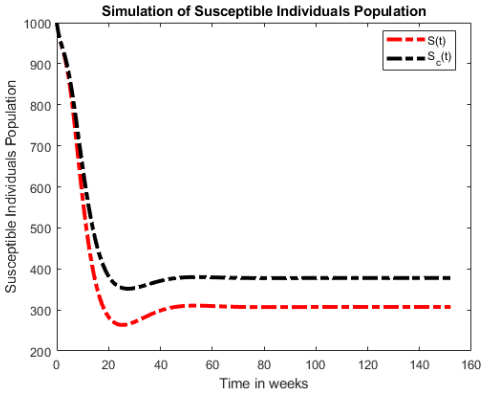

(a) $S(t)$

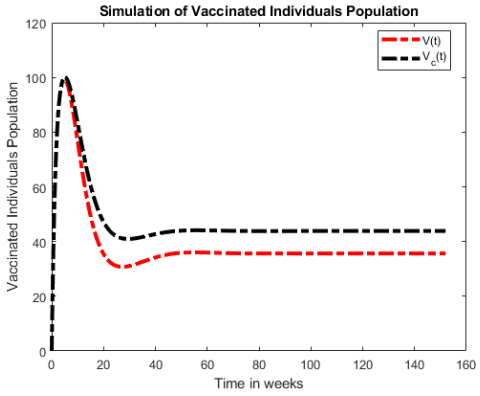

(b) $V(t)$

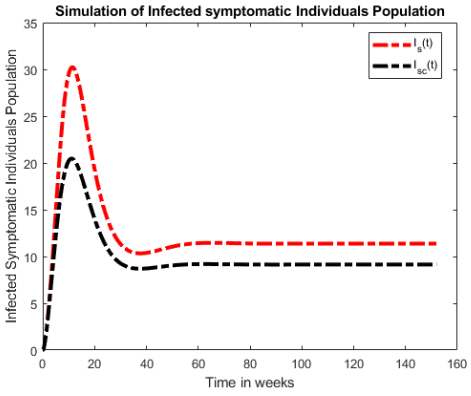

(c) $I_s(t)$

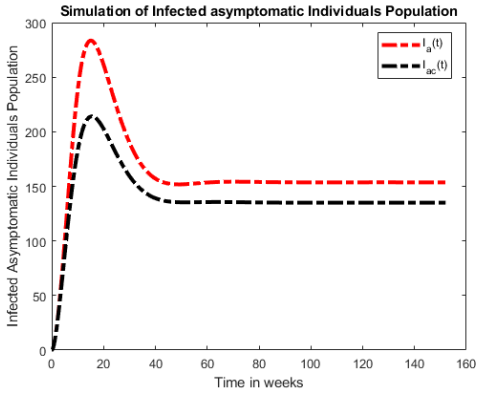

(d) I_a

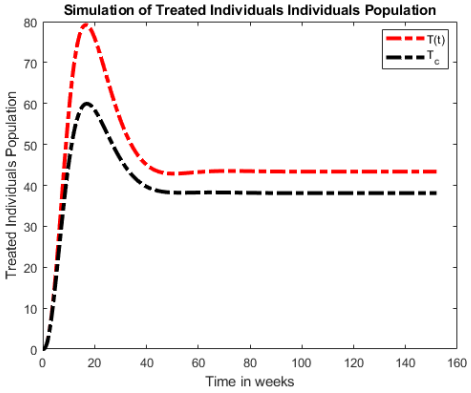

(e) $T(t)$

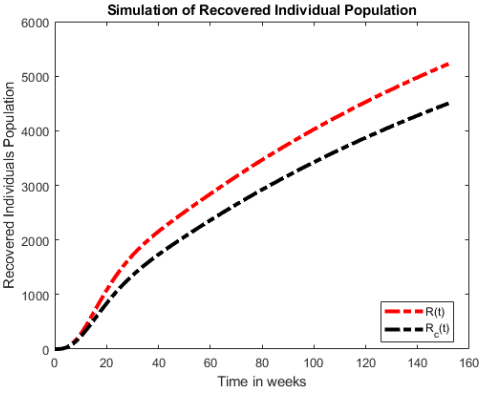

(f) $R(t)$

Figure 5.1: Simulation of the population of individuals in each compartment in the absence and presence of optimal control $S(t), S_c(t),\ V(t), V_c(t),\ I_s(t), I_{sc}(t),\ I_a(t), I_{ac}(t),\ T(t), T_c(t),$ $R(t), R_c(t),\ B(t)$ and $B_c(t)$ based on parameter values in Table 4.1.

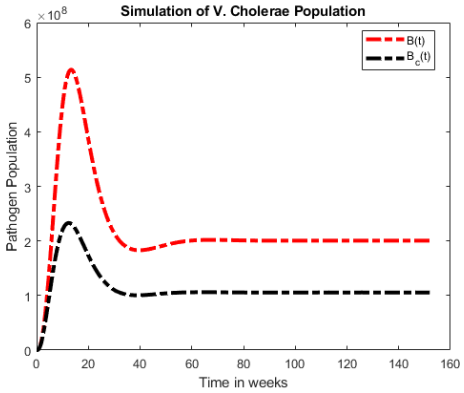

Figure 5.2: Simulation of the pathogen population in the absence and presence of optimal control $B(t)$ and $B_c(t)$ based on parameter values in Table 4.1.

A comparison of trajectories in the presence and absence of optimal control reveals that, as depicted in Figure 5.1a, susceptible individuals increase in the presence of optimal control. Similarly, vaccinated individuals' trajectory increases in the presence of optimal control (see Figure 5.1b). Figure 5.1c shows that population of infectious symptomatic individuals reduces in the presence of optimal control, an indication of effectiveness of control in reducing infections. Similarly, population of infectious asymptomatic reduces in the presence of optimal control (see Figure 5.1d). Lastly, population of treated individuals reduces in the presence of optimal control (see Figure 5.1e) and population of recovered individuals also reduces as indicated in Figure 5.1f. The pathogen population in the presence of optimal control also reduces (see Figure 5.2).

Chapter 6

Concluding remarks

Cholera is a historically feared diarrheal disease that affects different regions of the world, imposing serious economic constraints, especially in developing countries. Consequently, cholera cases have been reported worldwide and are a burden to humanity. As a result, countries have made efforts to prevent and respond to cholera outbreaks. Still, many concerns remain about the growing number of vulnerable people living in unsanitary conditions. Cholera is a waterborne disease and, more generally, an environmentally mediated human disease. As a result, cholera dynamics are controlled by human behaviour and other societal factors such as water, sanitary systems and environmental conditions. Such factors make it possible to model the disease.

Cholera epidemics have ravaged humanity since the 19^{th} century. An epidemic occurs when the number of reported infection cases is more than expected. Cholera is a scourge in Third World countries and remains a serious threat to public health and safety. Thus, it is paramount to continue researching and developing epidemiological models to control cholera epidemics effectively.

In the present research, the SIR model has been extended to include vaccinated individuals in place of those exposed. This is in line with curbing the cholera outbreak spread. A stability analysis of the model based on $\mathcal{R}_C$ for disease-free and endemic equilibrium showed $\mathcal{R}_C \leq 1$ and $\mathcal{R}_C \geq 1$ respectively. This implies that the epidemic could be eradicated when $\mathcal{R}_C \leq 1$ or spread in the population when $\mathcal{R}_C \geq 1$. Sensitivity analysis of parameters in $\mathcal{R}_C$ indicated

that ingestion rate β greatly influences $\mathcal{R}_C$. This means that the optimal control points should be based on reducing ingestion rate of cholera pathogens. A reduction of ingestion rate of the pathogen reduces $\mathcal{R}_C$ to 0.3133 down from $\mathcal{R}_C = 1.5665$. This indicated that an extension of control based on these facts would be promising.

The model has also been extended to include possible optimal control strategies such as hygiene and improved sanitation. Graphical simulations indicated that the number of infected individuals reduces when controls are in place to reduce ingestion of cholera pathogens. Such an observation implies that optimal control was effective. For future work, there is need to consider a model where different cholera strains are studied.

REFERENCES

[1] Agarwal, M., and Verma, V. Modeling and analysis of the spread of an infectious disease cholera with environmental fluctuations. *Applications and Applied Mathematics: An International Journal (AAM) 7*, 1 (2012), 27.

[2] Al-Tawfiq, J. A., Chopra, H., Dhama, K., Sah, R., Schlagenhauf, P., and Memish, Z. A. The cholera challenge: How should the world respond? *New Microbes and New Infections 51* (2023).

[3] Ali, M., Nelson, A. R., Lopez, A. L., and Sack, D. A. Updated global burden of cholera in endemic countries. *PLoS neglected tropical diseases 9*, 6 (2015), e0003832.

[4] Aligaz, A. A., and Munganga, J. M. W. Mathematical modelling of the transmission dynamics of contagious bovine pleuropneumonia with vaccination and antibiotic treatment. *Journal of Applied Mathematics 2019* (2019).

[5] Allen, L. J., Brauer, F., Van den Driessche, P., and Wu, J. *Mathematical epidemiology*, vol. 1945. Springer, 2008.

[6] Andam, E. A., Obiri-Apraku, L., Agyei, W., and Obeng-Denteh, W. Modeling cholera dynamics with a control strategy in ghana. *British Journal of Research 2*, 1 (2015), 031–041.

[7] Aron, J. L., et al. Mathematical modeling: the dynamics of infection. *Infectious disease epidemiology: Theory and practice* (2000).

[8] Arsie, A., and Ebenbauer, C. Refining lasalle's invariance principle. In *2009 American Control Conference* (2009), IEEE, pp. 108–112.

[9] Badshah, V., Porwal, P., and Tiwari, V. Mathematical modelling and role of dynamics in epidemiology. *International Journal of Computational Science and Mathematics 5*, 1 (2013), 4–10.

[10] Bayleyegn, Y. N. Mathematical analysis of a model of cholera transmission dynamics. Master's thesis, For Africa Institute of Mathematical Sciences (AIMS), 2009.

[11] Bebernes, J. The stability of dynamical systems (j.p. lasalle). *SIAM Review 21*, 3 (1979), 418–420.

[12] Berkovitz, L. D. Wendell h. fleming and raymond w. rishel, deterministic and stochastic optimal control. *Bulletin of the American Mathematical Society 82*, 6 (1976), 869–870.

[13] Bokil, U. A. Introduction to mathematics of infectious diseases. Tech. rep., Oregon State University, 2007.

[14] Brauer, F., Castillo-Chavez, C., Feng, Z., et al. *Mathematical models in epidemiology*, vol. 32. Springer, 2019.

[15] Bubniakova, L. *The Mathematics of Infectious Diseases*. Phd thesis, Univerzita Komenského» Fakulta matematiky, fyziky a informatiky» Katedra matematickej analỳzy a numerickej matematiky, 814 99 Bratislava 1, June 2007.

[16] Buie, T., Campbell, D. B., Fuchs III, G. J., Furuta, G. T., Levy, J., Vandewater, J., Whitaker, A. H., Atkins, D., Bauman, M. L., Beaudet, A. L., et al. Evaluation, diagnosis, and treatment of gastrointestinal disorders in individuals with asds: a consensus report. *Pediatrics 125*, Supplement_1 (2010), S1–S18.

[17] Bundi, M., Shah, M. M., Odoyo, E., Kathiiko, C., Wandera, E., Miring'u, G., Guyo, S., Langat, D., Morita, K., and Ichinose, Y. Characterization of vibrio cholerae o1 isolates responsible for cholera outbreaks in kenya between 1975 and 2017. *Microbiology and immunology 63*, 9 (2019), 350–358.

[18] Bundi, M. M. Characterization of toxigenic *Vibrio cholerae* isolates from kenya, 2007-2010. Master's thesis, School of Pure and Applied Sciences of Kenyatta University, Kenya, December 2012.

[19] Chao, L. Dennis, l. m. j., and Glenn Morris, J. J. Modeling cholera outbreaks. *Current Topics in Microbiology and Immunology: Spring-Verlag Berlin Heidelberg* (2013).

[20] Charnley, G. E., Yennan, S., Ochu, C., Kelman, I., Gaythorpe, K. A., and Murray, K. A. Cholera past and future in nigeria: Are the global task force on cholera control's 2030 targets achievable? *PLOS Neglected Tropical Diseases 17*, 5 (2023), e0011312.

[21] Codeço, C. T. Endemic and epidemic dynamics of cholera: the role of the aquatic reservoir. *BMC Infectious diseases 1* (2001), 1–14.

[22] Connor, B. A., Dawood, R., Riddle, M. S., and Hamer, D. H. Cholera in travellers: A systematic review. *Journal of travel medicine 26*, 8 (2019), 1–8.

[23] Cowman, G., Otipo, S., Njeru, I., Achia, T., Thirumurthy, H., Bartram, J., and Kioko, J. Factors associated with cholera in kenya, 2008-2013. *Pan African Medical Journal 28*, 1 (2017), 156–156.

[24] Crichton, N., and Mulhall, A. Epidemiology and health. In *Health Studies: An Introduction*. Springer, 2022, pp. 49–83.

[25] Crooks, A. T., and Hailegiorgis, A. B. An agent-based modeling approach applied to the spread of cholera. *Environmental Modelling & Software 62* (2014), 164–177.

[26] Davenport, R. J., Satchell, M., and Shaw-Taylor, L. M. W. Cholera as a sanitary test of british cities, 1831–1866. *The History of the Family 24*, 2 (2019), 404–438.

[27] davis, w. Two Models for Indirectly Transmitted Diseases: Cholera. Master's thesis, Department of Mathematical and Statistical Sciences at the University of Alberta, Edmonton, Canada, 2012.

[28] Desai, S. N., Cravioto, A., Sur, D., and Kanungo, S. Maximizing protection from use of oral cholera vaccines in developing country settings: an immunological review of oral cholera vaccines. *Human vaccines & immunotherapeutics 10*, 6 (2014), 1457–1465.

[29] Dimitrov, N. B., and meyers, L. A. Mathematical apapproach to infectious disease prediction and control. Tech. rep., Operations Research Department, Natural postgraduate, Monterey, Califonia.

[30] D'Mello-Guyett, L., Gallandat, K., Van den Bergh, R., Taylor, D., Bulit, G., Legros, D., Maes, P., Checchi, F., and Cumming, O. Prevention and control of cholera with household and community water, sanitation and hygiene (wash) interventions: a scoping review of current international guidelines. *PLoS One 15*, 1 (2020), e0226549.

[31] Emch, M., Feldacker, C., Islam, M. S., and Ali, M. Seasonality of cholera from 1974 to 2005: a review of global patterns. *International journal of health geographics 7*, 1 (2008), 1–13.

[32] Emvudu, y., and Kokomo, e. Stability analysis of cholera epidemic model of a closed population. *Journal of Applied Mathematics and Bioinformatics 2*, 1 (2012), 69–97. International Scientific Press.

[33] Fister, K. R., Gaff, H., Schaefer, E., Buford, G., and Norris, B. Investigating cholera using an sir model with age-class structure and optimal control. *Involve, A Journal of Mathematics 9*, 1 (2015), 83–100.

[34] Freedman, H. I., Ruan, S., and Tang, M. Uniform persistence and flows near a closed positively invariant set. *Journal of Dynamics and Differential Equations 6*, 4 (1994), 583–600.

[35] Fung, I. C. Cholera transmission dynamic models for public health practitioners. *Emerging themes in epidemiology 11* (2014), 1–11.

[36] Grad, Y. H., Miller, J. C., and Lipsitch, M. Cholera modeling: Challenges to quantitative analysis and predicting the impact of interventions. *Epidemiology (Cambridge, Mass.) 23*, 4 (2012), 523.

[37] Hailegiorgis, a., and Crooks, a. t. Agent-based Modelling for Humanitarian Issues: Disease and Refugee Camps. Tech. rep., Centre for Social Complexity, Krasnow Institute for Advanced Study, George Mason University, 2012.

[38] Hailemariam Hntsa, K., and Nerea Kahsay, B. Analysis of cholera epidemic controlling using mathematical modeling. *International Journal of Mathematics and Mathematical Sciences 2020* (2020).

[39] Hammer, W. H. Epidemic disease in england-the evidence of variability and of persistence of type. *The Lancet 1* (1906), 733–739.

[40] Haran, M. An introduction to models for disease dynamics. *Spartial Epidemiology, SAMSI* (2009).

[41] Harris, J. B., LaRocque, R. C., Chowdhury, F., Khan, A. I., Logvinenko, T., Faruque, A. S., Ryan, E. T., Qadri, F., and Calderwood, S. B. Susceptibility to vibrio cholerae infection in a cohort of household contacts of patients with cholera in bangladesh. *PLoS neglected tropical diseases 2*, 4 (2008), e221.

[42] Hartley, D. M., Morris Jr, J. G., and Smith, D. L. Hyperinfectivity: a critical element in the ability of v. cholerae to cause epidemics? *PLoS medicine 3*, 1 (2006), e7.

[43] Hartley, D. M., Morris Jr, J. G., and Smith, D. L. Hyperinfectivity: a critical element in the ability of v. cholerae to cause epidemics? *PLoS medicine 3*, 1 (2006), e7.

[44] Heesterbeek, J., and Roberts, M. The type-reproduction number t in models for infectious disease control. *Mathematical biosciences 206*, 1 (2007), 3–10.

[45] Howard-Jones, N. Robert koch and the cholera vibrio: a centenary. *British medical journal (Clinical research ed.) 288*, 6414 (1984), 379.

[46] Howe, M. G. *Man, Environment and Diseases in Brutain.* Penguin Books Ltd, England, 1973.

[47] Ilic, I., and Ilic, M. Global patterns of trends in cholera mortality. *Tropical Medicine and Infectious Disease 8*, 3 (2023), 169.

[48] Ioffe, A. D., and Tihomirov, V. M. *Theory of extremal problems: Theory of Extremal Problems.* Elsevier, 2009.

[49] Ionides, E. L., Bretó, C., and King, A. A. Modeling disease dynamics: Cholera as a case study, 2008.

[50] Jeffrey, O. M. A mathematical model for the transmission dynamics of cholera with control strategy. *International Journal Of Science and Technology Volume 2 No. 11, November* (2013).

[51] Joh, R. I., Wang, H., Weiss, H., and Weitz, J. S. Dynamics of indirectly transmitted infectious diseases with immunological threshold. *Bulletin of mathematical biology 71* (2009), 845–862.

[52] Johnson, t. Mathematical Modeling of Diseases: Susceptible-Infected-Recovered (SIR) Model. Math 4901 Senior Seminar, University of Minnesota, Morris, Spring 2009.

[53] Kadaleka, s. Assessing the Effects of Nutrition and Treatment in Cholera Dynamics: The Case of Malawi. Master's thesis, School of Mathematical Sciences, University of Dar es Salaam, Tanzania, 2011.

[54] Keeling, M. J., and Rohani, P. *Modeling infectious diseases in humans and animals.* Princeton university press, 2011.

[55] Kermack, W. O., and McKendrick, A. G. A contribution to the mathematical theory of epidemics. *Proceedings of the royal society of london. Series A, Containing papers of a mathematical and physical character 115*, 772 (1927), 700–721.

[56] Kraay, A. Methodology for a world bank human capital index. *World Bank Policy Research Working Paper*, 8593 (2018).

[57] LaRocque, R., and Harris, J. B. Cholera: clinical features, diagnosis, treatment, and prevention. *This Top. Available online: https://www. uptodate. com/contents/cholera-clinical-features-diagnosis-treatment-and-prevention (accessed on 20 September 2022)* (2018).

[58] Lee, K. The global dimensions of cholera. *Global Change and Human Health 2*, 1 (2001), 6–17.

[59] Li, M. Y., Graef, J. R., Wang, L., and Karsai, J. Global dynamics of a seir model with varying total population size. *Mathematical biosciences 160*, 2 (1999), 191–213.

[60] Liao, S., and Wang, J. Global stability analysis of epidemiological models based on volterra–lyapunov stable matrices. *Chaos, Solitons & Fractals 45*, 7 (2012), 966–977.

[61] Lin, C., and Wen, T. How spatial epidemiology helps understand infectious human disease transmission. *Tropical Medicine and Infectious Disease 7*, 8 (2022), 164.

[62] Lukes, D. L. *Differential equations: classical to controlled*. Academic Press, 1982.

[63] Mabotsa, M., Munganga, J. M. W., and Hassan, A. S. Mathematical modelling and optimal control of the transmission dynamics of enterovirus. *Physica Scripta 97*, 3 (2022), 4–52.

[64] Mahalanabis, D., Molla, A., and Sack, D. A. Clinical management of cholera. In *Cholera*. Springer, 1992, pp. 253–283.

[65] Mahalanabis, D., Molla, A. M., and Sack, D. A. Clinical Management of Cholera. In *Cholera*, Dhiman Barua and W. B. Greenough (III), Ed. Springer, Plenum Medical Company, New York, 1992, pp. 253–283.

[66] Mahamud, A. S., Ahmed, J. A., Nyoka, R., Auko, E., Kahi, V., Ndirangu, J., Nguhi, M., Burton, J. W., Muhindo, B. Z., Breiman, R. F., et al. Epidemic cholera in kakuma refugee camp, kenya, 2009: the importance of sanitation and soap. *The Journal of Infection in Developing Countries 6*, 03 (2012), 234–241.

[67] Mandal, S., Mandal, M. D., and Pal, N. K. Cholera: a great global concern. *Asian Pacific journal of tropical medicine 4*, 7 (2011), 573–580.

[68] Mengel, M. A., Delrieu, I., Heyerdahl, L., and Gessner, B. D. Cholera outbreaks in africa. *Cholera outbreaks* (2014), 117–144.

[69] Millet, Y. A., Alvarez, D., Ringgaard, S., von Andrian, U. H., Davis, B. M., and Waldor, M. K. Insights into vibrio cholerae intestinal colonization from monitoring fluorescently labeled bacteria. *PLoS pathogens 10*, 10 (2014), e1004405.

[70] Mintz, E. D., and Tauxe, R. V. Cholera in africa: a closer look and a time for action. *The Journal of infectious diseases 208*, suppl_1 (2013), S4–S7.

[71] Momanyi, M. R. Phenotypic and molecular characterization of vibrio cholerae isolated from cholera outbreaks in western kenya. Master's thesis, Biotechnology, Jomo Kenyatta University of Agriculture and Technology, 2010.

[72] Motta, S., and Pappalardo, F. Mathematical modeling of biological systems. *Briefings in Bioinformatics 14*, 4 (2013), 411–422.

[73] Mukandavire, Z., Liao, S., Wang, J., Gaff, H., Smith, D. L., and Morris, J. G. Estimating the reproductive numbers for the 2008–2009 cholera outbreaks in Zimbabwe. *Proceedings of the National Academy of Sciences 108*, 21 (2011), 8767–8772.

[74] Munnaf, M. F. *Installation of Simple Water Treatment Unit at Cyclone-Aila Affected Koyra Region and Assessment of DALYs Lost due to Diarrhoea.* PhD thesis, Khulna University of Engineering & Technology (KUET), Khulna, Bangladesh, 2016.

[75] Mutreja, A., Kim, D. W., Thomson, N. R., Connor, T. R., Lee, J. H., Kariuki, S., Croucher, N. J., Choi, S. Y., Harris, S. R., Lebens, M., et al. Evidence for several waves of global transmission in the seventh cholera pandemic. *Nature 477*, 7365 (2011), 462–465.

[76] Nelson, E. J., Harris, J. B., Glenn Morris Jr, J., Calderwood, S. B., and Camilli, A. Cholera transmission: the host, pathogen and bacteriophage dynamic. *Nature Reviews Microbiology 7*, 10 (2009), 693–702.

[77] Nguyen, C., and Carlson, J. M. Optimizing real-time vaccine allocation in a stochastic sir model. *PloS one 11*, 4 (2016), e0152950.

[78] Ochoche, J. M. A Mathematical Model for the Transmission Dynamics of Cholera with Control Strategy. *International Journal of Science and Technology 2*, 11 (2013), 797–803.

[79] Onuorah, M. O., Atiku, F., and Juuko, H. Mathematical model for prevention and control of cholera transmission in a variable population. *Research in Mathematics 9*, 1 (2022).

[80] Organization, W. H., et al. Weekly bulletin on outbreaks and other emergencies: Week 42: 14–20 october 2017. *Weekly Bulletin on Outbreaks and other Emergencies* (2017), 1–7.

[81] Oz, Y., Rubinstein, I., and Safra, M. Superspreaders and high variance infectious diseases. *Journal of Statistical Mechanics: Theory and Experiment 2021*, 3 (2021), 033417.

[82] Pascual, M., Bouma, M. J., and Dobson, P. A. Cholera and climate: revisiting the quantitative evidence. *Microbes and Infection 4* (2002), 237–245.

[83] Paul, J. Introduction to infectious diseases. In *Disease Causing Microbes*. Springer, 2024, pp. 1–63.

[84] Paverifontana, S., and Capasso, V. A mathematical model for the cholera epidemic in the european mediterranean region. *Rev.Epidemic.Sante Publ* (1979).

[85] Peak, C. M., Reilly, A. L., Azman, A. S., and Buckee, C. O. Prolonging herd immunity to cholera via vaccination: Accounting for human mobility and waning vaccine effects. *PLoS neglected tropical diseases 12*, 2 (2018), e0006257.

[86] Qadri, F., Ali, M., Lynch, J., Chowdhury, F., Khan, A. I., Wierzba, T. F., Excler, J.-L., Saha, A., Islam, M. T., Begum, Y. A., et al. Efficacy of a single-dose regimen of inactivated whole-cell oral cholera vaccine: results from 2 years of follow-up of a randomised trial. *The Lancet Infectious Diseases 18*, 6 (2018), 666–674.

[87] Rabbani, G., and Greenough III, W. Food as a vehicle of transmission of cholera. *Journal of diarrhoeal diseases research* (1999), 1–9.

[88] Ramamurthy, T., and Ghosh, A. A re-look at cholera pandemics from early times to now in the current era of epidemiology. *Journal of Disaster Research 16*, 1 (2021), 110–117.

[89] Safi, M. A., Melesse, D. Y., and Gumel, A. B. Dynamics analysis of a multi-strain cholera model with an imperfect vaccine. *Bulletin of mathematical biology 75*, 7 (2013), 1104–1137.

[90] Said, M. D., et al. *Epidemic cholera in KwaZulu-Natal: The role of the natural and social environment*. PhD thesis, University of Pretoria, 2006.

[91] Sanches, R. P., Ferreira, C. P., and Kraenkel, R. A. The role of immunity and seasonality in cholera epidemics. *Bulletin of Mathematical Biology 73* (2011), 2916–2931. Society of Mathematical Biology, 2011.

[92] Shuai, Z., and van den Driessche, P. Global stability of infectious disease models using lyapunov functions. *SIAM Journal on Applied Mathematics 73*, 4 (2013), 1513–1532.

[93] Siegel, F. R. *Cities and mega-cities: problems and solution strategies.* Springer, 2018.

[94] Smith, H. L., and Waltman, P. *The theory of the chemostat: dynamics of microbial competition*, vol. 13. Cambridge university press, 1995.

[95] Snow, S. J. John snow md (1813–1858). part ii: Becoming a doctor his medical training and early years of practice. *Journal of medical biography 8*, 2 (2000), 71–77.

[96] Stoltzfus, J. D., Carter, J. Y., Akpinar–elci, M., Matu, M., Kimotho, V., Giganti, M. J., Langat, D., and Elci, O. C. Interaction between climatic, environmental, and demographic factors on cholera outbreaks in Kenya. *Infectious Diseases of Poverty 3*, 37 (October 2014). BioMed Central.

[97] Stuart, A., and Humphries, A. R. *Dynamical systems and numerical analysis*, vol. 2. Cambridge University Press, 1998.

[98] Sun, G., Xie, J., Huang, S., Jin, Z., Li, M., and Liu, L. Transmission dynamics of cholera: Mathematical modeling and control strategies. *Communications in Nonlinear Science and Numerical Simulation 45* (2017), 235–244.

[99] Taylor, D. L., Kahawita, T. M., Cairncross, S., and Ensink, J. H. The impact of water, sanitation and hygiene interventions to control cholera: a systematic review. *PLoS one 10*, 8 (2015), e0135676.

[100] Tian, J., Liao, S., and Wang, J. Dynamical analysis and control strategies in modeling cholera. *A monograph* (2010), 1–21.

[101] Tian, J. P., and Wang, J. Global stability for cholera epidemic models. *Mathematical biosciences 232*, 1 (2011), 31–41.

[102] Tianyou, Z. Contact network based framework for infectious disease interventions. Master's thesis, Computing Engineering, 2014.

[103] Tuite, A. R., Tien, J., Eisenberg, M., Earn, D. J., Ma, J., and Fisman, D. N. Cholera epidemic in haiti, 2010: using a transmission model to explain spatial spread of disease and identify optimal control interventions. *Annals of internal medicine 154*, 9 (2011), 593–601.

[104] Tulchinsky, T. H., and Varavikova, E. A. Environmental and occupational health. *The New Public Health* (2014), 471.

[105] Van den Driessche, P., and Watmough, J. Reproduction numbers and sub-threshold endemic equilibria for compartmental models of disease transmission. *Mathematical biosciences 180*, 1-2 (2002), 29–48.

[106] Van den Driessche, P., Watmough, J., Brauer, F., and Wu, J. Mathematical epidemiology. lecture notes in mathematics. Tech. rep., 2008.

[107] Wang, J., and Modnak, C. Modeling cholera dynamics with controls. *Canadian Applied Mathematics Quarterly 19*, 3 (2011).

[108] Weil, A. A., Begum, Y., Chowdhury, F., Khan, A. I., Leung, D. T., LaRocque, R. C., Charles, R. C., Ryan, E. T., Calderwood, S. B., Qadri, F., et al. Bacterial shedding in household contacts of cholera patients in dhaka, bangladesh. *The American journal of tropical medicine and hygiene 91*, 4 (2014), 738.

[109] Wendelboe, A. M., Grafe, C., and Carabin, H. The benefits of transmission dynamics models in understanding emerging infectious diseases. *The American journal of the medical sciences 340*, 3 (2010), 181–186.

[110] Willeberg, P., Paisley, L., Lind, P., et al. Epidemiological models to support animal disease surveillance activities. *Rev. sci. tech. Off. int. Epiz 30*, 2 (2011), 603–614.

[111] Winderman, E., Mejia, R., and Rogers, B. " all smell is disease": Miasma, sensory rhetoric, and the sanitary-bacteriologic of visceral public health. *Rhetoric of Health & Medicine 2*, 2 (2019), 115–146.

[112] World Health Organisation (WHO). Global Task Force on Cholera Control. Cholera Country Pofile: Kenya 2010.

[113] Yonatan H. Grad, J. C. M., and Lipsitch, M. Cholera modeling: Chaentionsllenges to quantitative analysis and predicting the inmpact of interventions. *Lippincott Williams and Wilkins Vol 23,* (2012).

Appendix A

Turnitin Report

Mathematical Modelling of the Transmission Dynamics of Cholera

ORIGINALITY REPORT

16%	14%	11%	3%
SIMILARITY INDEX	INTERNET SOURCES	PUBLICATIONS	STUDENT PAPERS

PRIMARY SOURCES

1	uir.unisa.ac.za Internet Source	10%
2	Malebese Mabotsa, Justin Manango W Munganga, Adamu Shitu Hassan. "Mathematical modelling and optimal control of the transmission dynamics of enterovirus", Physica Scripta, 2022 Publication	2%
3	Malebese Mabotsa, Justin Manango Wazute Munganga, Adamu Shitu Hassan. "Mathematical modelling and optimal control of the transmission dynamics of enterovirus", Physica Scripta, 2022 Publication	1%
4	www.irjmets.com Internet Source	1%
5	Mohammad A. Safi, Dessalegn Y. Melesse, Abba B. Gumel. "Dynamics Analysis of a Multi-strain Cholera Model with an Imperfect	1%